arXiv:astro-ph/9907402v1 28 Jul 1999

A Comparison of the Interiors of Jupiter and Saturn

Tristan Guillot
Observatoire de la Côte d'Azur
Laboratoire G.D. Cassini, CNRS UMR 6529
BP 4229
06304 Nice Cedex 4, France
E-mail: guillot@obs-nice.fr

Submitted December 12, 1998; Revised May 5, 1999

Planetary and Space Science, in press
Nantes Symposium special issue

Number of manuscript pages: 25 Number of tables: 6
Number of figures: 10

KEYWORDS: Jupiter, Saturn
Interiors, planets
Chemical abundances

RUNNING HEAD: Interiors of Jupiter and Saturn

Abstract

Interior models of Jupiter and Saturn are calculated and compared in the framework of the three-layer assumption, which rely on the perception that both planets consist of three globally homogeneous regions: a dense core, a metallic hydrogen envelope, and a molecular hydrogen envelope. Within this framework, constraints on the core mass and abundance of heavy elements (i.e. elements other than hydrogen and helium) are given by accounting for uncertainties on the measured gravitational moments, surface temperature, surface helium abundance, and on the inferred protosolar helium abundance, equations of state, temperature profile and solid/differential interior rotation.

Results obtained solely from static models matching the measured gravitational fields indicate that the mass of Jupiter's dense core is less than $14\,\mathrm{M}_\oplus$ (Earth masses), but that models with no core are possible given the current uncertainties on the hydrogen-helium equation of state. Similarly, Saturn's core mass is less than $22\,\mathrm{M}_\oplus$ but no lower limit can be inferred. The total mass of heavy elements (including that in the core) is constrained to lie between 11 and $42\,\mathrm{M}_\oplus$ in Jupiter, and 19 to $31\,\mathrm{M}_\oplus$ in Saturn. The enrichment in heavy elements of their *molecular* envelopes is 1 to 6.5, and 0.5 to 12 times the solar value, respectively.

Additional constraints from evolution models accounting for the progressive differentiation of helium (Hubbard et al. 1999) are used to obtain tighter, albeit less robust, constraints. The resulting core masses are then expected to be in the range 0 to $10\,\mathrm{M}_\oplus$, and 6 to $17\,\mathrm{M}_\oplus$ for Jupiter and Saturn, respectively. Furthermore, it is shown that Saturn's atmospheric helium mass mixing ratio, as derived from Voyager, $Y = 0.06 \pm 0.05$, is probably too low. Static and evolution models favor a value of $Y = 0.11 - 0.25$. Using, $Y = 0.16 \pm 0.05$, Saturn's molecular region is found to be enriched in heavy elements by 3.5 to 10 times the solar value, in relatively good agreement with the measured methane abundance.

Finally, in all cases, the gravitational moment J_6 of models matching all the constraints are found to lie between 0.35 and 0.38×10^{-4} for Jupiter, and between 0.90 and 0.98×10^{-4} for Saturn, assuming solid rotation. For comparison, the uncertainties on the measured J_6 are about 10 times larger. More accurate measurements of J_6 (as expected from the Cassini orbiter for Saturn) will therefore permit to test the validity of interior models calculations and the magnitude of differential rotation in the planetary interior.

1 Introduction

Jupiter and Saturn played a key role in the formation of the Solar System. Yet their internal structure and composition are still poorly known. This is due to the fact that the only way to probe the deep regions of these planets is by calculating interior models matching their observed gravitational field, a method that can only yield information on quantities that are averaged over a significant fraction of the planetary radius. It is however of primordial importance to derive the largest ensemble of theoretical models compatible with observations, and yet to try to narrow down the ensemble of solutions as much as possible, thus providing related scientific fields with useful constraints.

Previous work on the subject, including those of Hubbard & Marley (1989), Zharkov & Gudkova (1992), Chabrier et al. (1992) and Guillot et al. (1994b), has generally aimed at finding a sample of models matching the observational constraints, i.e. radius and gravitational moments. Using the new H/He mixing ratio from Galileo and taking advantage of the improvements in computing capabilities over the past years, Guillot et al. (1997) have calculated an extended ensemble of interior models of Jupiter matching all observational constraints within the error bars.

Although new observations of Saturn relevant to studies of its internal structure will probably have to await the arrival of the Cassini-Huygens space mission in 2004, the present article is motivated by the renewed interest in giant planet formation subsequent to the discovery of extrasolar planets (see e.g. Mayor & Queloz 1995; Marcy and Butler 1998). As a consequence, the formation of giant planets by gas instability (Cameron 1978), which had been abandoned to the profit of the nucleated instability model (Lissauer 1993, Pollack et al. 1996), has reborn from its ashes, and been proposed as a mechanism that led to the rapid formation of Jupiter and Saturn (Boss 1998). This prompts for a recalculation of models of Saturn aimed at constraining its internal composition.

Furthermore, accurate evolution calculations (Guillot et al. 1995) using improved atmospheric models (Marley et al. 1996; Burrows et al. 1997) were available, but assumed a homogeneous structure. The additional energy provided by helium sedimentation (or that of any other element) has been estimated by Hubbard et al. (1999). The resulting model ages therefore provide an additional constraint, as they must, within the uncertainties, agree with the age of the Solar System.

The aim of the present article is thus to calculate new static models of Saturn, to include additional constraints obtained from evolution calculations on the models of Jupiter and Saturn, and to compare the structure and composition of the two giant planets. Relevant observations and input physics are presented in Section 2. The main assumption of a three layer structure for Jupiter and Saturn is discussed in Section 3. I then present in the next section the method used to calculate interior models. The results are detailed in Section 5; their consequences on models of the formation of the giant planets and perspectives are discussed in Section 6.

2 Input data

2.1 Gravitational field

Jupiter and Saturn are rapid rotators: the rotation rates derived from their magnetic fields are 9 hours and 55 minutes, and 10 hours and 39 minutes, respectively. Although the consequences of rotation on their very structure, and in particular the presence and strength of convection in their interiors, are difficult to assess (Stevenson and Salpeter 1977; see also Busse 1976, Zhang & Schubert 1996), this property is a chance because it allows us to constrain their interior density profiles, by measuring the departures from sphericity of their gravitational potentials:

$$U(r,\theta)=\frac{GM}{r}\left\{1-\sum_{i=1}^{\infty}\left(\frac{R_{\rm eq}}{r}\right)^{2i}J_{2i}P_{2\rm i}(\cos\theta)\right\}, \tag{1}$$

where G is the gravitational constant, M the mass of the planet, $R_{\rm eq}$ its equatorial radius, r the distance to the planetary center, θ the polar angle (to the rotation axis), and $P_{2\rm i}$ are Legendre polynomials. The J_{2i} are the gravitational moments. Their observed values (inferred mostly from the trajectories of the Pioneer and Voyager spacecrafts) are given in Table I. The gravitational moments can also be related to the internal density profile $\rho(r)$ (and thus to theoretical models) by the following relation (e.g., Zharkov & Trubitsyn 1974):

$$J_{2i}=-\frac{1}{MR_{\rm eq}^{2i}}\int\rho(r)r^{2i}P_{2i}(\cos\theta)d\tau, \tag{2}$$

in which the integral is calculated over the total volume of the planet. A common method for the solution of Eq. 2 is the so-called theory of figures, which will not be developed here (see Zharkov & Trubitsyn 1978). The present work uses equations to the third order of the theory of figures.

Table I: Characteristics of the gravitational fields

	Jupiter		Saturn	
	measured[a]	adjusted[c]	measured[b]	adjusted[c]
$M/\mathrm{M}_\oplus$	317.83		95.147	
$R_{\rm eq}/10^9$	7.1492(4)		6.0268(4)	
$J_2/10^{-2}$	1.4697(1)	1.4682(1)	1.6332(10)	1.6252(10)
$J_4/10^{-4}$	$-5.84(5)$	$-5.80(5)$	$-9.19(40)$	$-8.99(40)$
$J_6/10^{-4}$	0.31(20)	0.30(20)	1.04(50)	0.94(50)

Note. The numbers in parentheses are the uncertainty in the last digits of the given value. All the quantities are relative to the 1 bar pressure level.

[a] Campbell & Synnott (1985).

[b] Campbell & Anderson (1989).

[c] Adjusted for differential rotation using Hubbard (1982).

A complication arises from the fact that the equations derived from that theory generally assume the planet to be rotating as a solid body. Observations of the atmospheric winds show significant variations with latitude, however (e.g., Gierasch & Conrath 1993). The question of the depth to which these differential rotation patterns extend is still open. Hubbard (1982) has proposed a solution to the planetary figure problem in the case of a deep rotation field that possesses cylindrical symmetry. It is thus possible to derive, from interior models assuming solid rotation, the value of the gravitational moments that the planet would have if its surface rotation pattern extended deep into its interior. It is *a priori* impossible to prefer one model to the other, and I will therefore present calculations assuming both solid and differential rotation. Table I gives both the measured gravitational moments, and those corrected for differential rotation.

2.2 Atmospheric abundances

The following definitions for chemical abundances will be used: X, Y and Z are the mass mixing ratios of hydrogen, helium, and heavy elements, respectively. Because it is difficult to separate helium and heavy elements, I also introduce an *equivalent* helium mass mixing ratio, $Y_Z \sim Y + Z$ (see Eq. 10 hereafter for an exact derivation).

A first indicator of the internal evolution of the giant planets is the abundance of helium in their atmospheres. Since the helium to hydrogen ratio in the whole planet must have remained constant for its entire evolution, any measured depletion in the atmosphere compared to the initial value means that more helium is present deeper inside the planet. This has significant consequences on the planet's internal structure and evolution. Unfortunately, the initial (i.e., protosolar) helium mass mixing ratio cannot be directly inferred from abundance measurements in the solar photosphere because of the progressive gravitational settling of helium into the radiative zone of our star. Instead, determination of the protosolar value must rely on solar evolution models including diffusion and satisfaction of the constraints provided by observations of solar oscillations. These indicate that the protosolar helium mass mixing ratio was $Y/(X + Y) = 0.270 \pm 0.005$ (Bahcall & Pinsonneault 1995).

In situ measurements of that quantity in Jupiter yield $Y/(X + Y) = 0.238 \pm 0.007$ (von Zahn et al. 1998). Combined radio occultation measurements and spectra analysis indicate that, in Saturn, $Y/(X+Y) = 0.06 \pm 0.05$ (Conrath et al. 1984). However, similar measurements for Jupiter led to $Y/(X + Y) = 0.18 \pm 0.04$ (Gautier et al. 1982), in disagreement with the value obtained by the Galileo probe. It is conceivable that the value obtained for Saturn is incorrect too, prompting us to consider other values for the atmospheric helium mixing ratio in that planet. Indeed, both a reexamination of Voyager IRIS data (Gautier & Conrath, personal communication 1998) and constraints from the static and evolutionary models (see below, and accompanying paper by Hubbard et al. 1999) point to significantly higher values of Y. In any case, the conclusion that more helium was present in the protosolar nebula gas from which Jupiter and Saturn formed than is observed today in their atmospheres seems inescapable. This is explained by the presence of either a first order molecular/metallic phase transition of hydrogen, or a hydrogen/helium phase separation, or both, as described below.

The measured abundances of other elements also provide important clues to the composition of the planets. Both Jupiter and Saturn are globally enriched in heavy elements compared to the Sun. In Jupiter, the *in situ* measurements of the Galileo probe are compatible with a ∼3 times solar enrichment of carbon and sulfur (Niemann et al. 1998). It is still unclear as to whether nitrogen is close to solar (by a factor 1 to 1.5; de Pater and Massie 1985), moderately (2.2 to 2.4; Carlson et al. 1992) or strongly enriched (3.5 to 4.5 times solar; Folkner et al. 1998). Water is still a problem because of its condensation at deep levels, and only a lower limit of ∼0.1 times solar can be inferred from the measurements. On the contrary, neon, and perhaps argon appear to be depleted, having abundances less than 0.13 and 1.7 times solar, respectively (Niemann et al. 1998). This might be due to the fact that noble gases, in particular neon, tend to be carried deep into the interior by helium-rich droplets (Roulston & Stevenson 1995).

Unfortunately, the uncertainties for Saturn are still relatively large. Its atmosphere is enhanced in carbon by a factor of 2 to 7, and in nitrogen by a factor 2 or more (Gautier & Owen 1989). Observationally, it could therefore be more rich in heavy elements than the jovian atmosphere. This will be tested by the Cassini-Huygens mission.

2.3 Atmospheric temperatures

The temperatures at the tropopause (at pressures of about 0.3 bar) are relatively well constrained by direct inversions of infrared spectra. These predict relatively large latitudinal temperature changes of the order of 10 K (Conrath et al. 1989). The temperature gradients decrease with tropospheric depth, as interior convection presumably becomes more efficient in redistributing the heat. However, the accuracy of this method drops rapidly with increasing pressure and does not reach levels deep enough to be used as surface condition for interior models. So far, the only reliable measurement of the deep tropospheric temperature of a giant planet is that from the Galileo probe in Jupiter: 166 K at 1 bar (Seiff et al. 1998). It is not clear however how representative of the whole planet this measurement is. Previous analyses have relied upon (local) radio occultation data acquired with the Pioneer and Voyager spacecrafts (Lindal et al. 1981, 1985) that predicted 1 bar temperatures of 165 ± 5 K in Jupiter and 134.8 ± 5K in Saturn. The temperatures inferred from these data are however dependent on the assumed mean molecular weight $\overline{m}$. In the case of a vertically uniform atmospheric composition (a fairly accurate representation in the present case), one can derive the temperature directly from the measured refractivity N as a function of altitude z:

$$T(z) = -\frac{\overline{m}}{k_{\rm B} N(z)} \int_{\infty}^{z} N(h) g(h) dh, \tag{3}$$

where g is the gravity and $k_{\rm B}$ is the Boltzmann constant.

The new measurement of the helium mixing ratio in Jupiter yields a higher $\overline{m}$, and hence a larger surface temperature of 170.4 K at 1 bar. On the other hand, the interpretation of the IRIS data suggests that the radio occultation data tend to predict temperatures that are too high by a few kelvins (Gautier, personal communication 1998), therefore pointing to a value closer to 165 K. In this work, I choose to consider values of 165 to 170 K for Jupiter.

In the case of Saturn, I will show that values of Y higher than the Voyager value ($Y = 0.06$), are more in agreement with the evolution of this planet, and that the surface helium mass mixing ratio could be as high as 0.25. According to Eq. 3, these high values indicate that the planet's surface temperature might be significantly underestimated, and be of the order of 145 K, a value that I choose to use in the calculations. I also present calculations with 1 bar temperatures of 135 K. The lower limit of 130 K appears to be inconsistent with the static and evolutionary constraints and is therefore not used.

2.4 Equations of state

Inside Jupiter and Saturn, all chemical species are compressed to very high pressures (up to 10-70 Mbar) at temperatures for which experimental data are difficult to obtain, and theoretical models very complex. Hydrogen undergoes a transition from a molecular phase at low pressures to a metallic phase at pressures larger than about one Mbar. Yet it is still unclear whether this transition is discontinuous (first order) or continuous.

To date, the most thorough theoretical effort to model the high-pressure, low-temperature liquid hydrogen equation of state (EOS) predicts that this element passes from molecular to metallic phase via a first order (i.e. discontinuous) plasma phase transition (PPT) (Saumon et al. 1995). This EOS is however based on the so-called "chemical picture" which assumes that the species considered (H, H_2, H^+, H^-) are chemically distinct under all conditions. This assumption is probably not entirely satisfied in the region of interest, and hence, Saumon et al.

(1995) provide two EOSs: a thermodynamically consistent one, which includes the PPT, and one that has been smoothly interpolated between low-pressure and high-pressure regimes. These two EOSs (referred to as "PPT-EOS" and "i-EOS" hereafter) are used in this work and serve as an estimate of present uncertainties on the calculated densities of hydrogen at high pressure.

Recent shock compression on liquid deuterium (e.g., Holmes et al. 1995; Weir et al. 1996; Collins et al. 1998) show that the molecular/metallic transition is even more complex than was expected. At pressures of about 1.4 Mbar, the resistivity of the liquid ceases to decrease, which is interpreted as the sign that the metal phase has been reached, thus favoring the case for a continuous molecular to metallic transition (Nellis et al. 1999; Da Silva et al. 1997). However, the measured resistivity is still larger than theoretical estimates pertaining to a fully-ionized metal (Hubbard et al. 1997). As discussed by Nellis et al. (1998), in the $1-2$ Mbar pressure range, the transition is from a semi-conducting to an essentially metallic fluid but one which retains a strong pairing character. As these authors note, "the precise mechanism by which a metallic state might be attained is still a matter of debate". One proposition is that the PPT exists, but lies deeper still (Saumon et al. 1999). The complex behavior of hydrogen due to the molecular/metallic transition probably extends over the range $1-3$ Mbar indicated in Fig. 2 hereafter.

Helium is the source of yet another difficulty: its behavior would be simpler than that of hydrogen, since it requires larger pressures to become ionized, were it not for its interactions with hydrogen atoms and molecules, and the subsequent possibility that a phase *separation* between helium-rich and helium-poor mixtures occurs in Jupiter and Saturn (Salpeter 1973). To date, no fully consistent equation of state including both hydrogen and helium has been made available. Attempts to predict the critical pressures and temperatures at which helium separates from hydrogen still yield very different results (Pfaffenzeller et al. 1995; Klepeis et al. 1991) but generally agree that this should take place in the metallic region (see also Stevenson 1982). I choose to consider this phase separation as a possibility, but do not attempt to derive a consistent phase-diagram. Instead, in the framework of the Saumon-Chabrier EOS, helium is added to hydrogen using the ideal mixing rule (thereby preventing any derivation of Gibbs' mixing enthalpy).

Heavier elements are present in smaller quantities, so that errors on their EOSs should not lead to substantial changes in the final interior models. Their contribution is derived from the ideal mixing rule, with the assumption that their EOS is proportional to that of helium, with a factor equal to the ratio between the molecular mass of helium and heavy elements. However, contrary to previous work (see Chabrier et al. 1992, Guillot et al. 1994b, 1997), I account for their specific heat, as it is significantly different from that of helium. The additional entropy due to the presence of heavy elements is derived within the perfect gas formalism. This is clearly an oversimplification, but this term is only significant in the molecular phase and not in the partly degenerate metallic phase, for which density is less sensitive to temperature changes. Accordingly, the specific entropy of the gas at any given temperature and pressure is written:

$$S(T,P,Y,Z) = XS_{\rm H}(P,T) + YS_{\rm He}(P,T) + S_{\rm mix}(P,T,Y) + Z\frac{k_{\rm B}}{m_z}\left[c_{p\,z}\ln\frac{T}{T_0} - \ln\frac{P}{P_0}\right], \quad (4)$$

where $S_{\rm H}$ and $S_{\rm He}$ are the entropies for pure hydrogen and helium, respectively, $S_{\rm mix}$ is the entropy of mixture of these two species (see Saumon et al. 1995), m_z is the (mean) molecular mass of the heavy elements, $c_{p\,z}k_{\rm B}$ their specific heat (in units of $\mathrm{erg\,K^{-1}\,g^{-1}}$) and T_0 and P_0 are arbitrary reference temperature and pressure, respectively. I use $c_{p\,z} = 4$ and $m_z = 17$ as typical values. Different values were tested without significantly changing the results. In fact, most of the difference with previous calculations is the result of the use of Y (i.e. in the molecular envelope, the observed helium mass mixing ratio) instead of the equivalent helium mass fraction Y_Z in Eq. 4 (see Guillot et al. 1994b). Note that in the molecular envelope, in which the temperature profile is most important, helium is in atomic form and has the smallest possible specific heat. The use of Eq. 4 is thus especially important for Saturn, whose molecular envelope is rich in heavy elements. The resulting models of this planet are substantially cooler than previous ones.

In the central cores of the planets, I use the density relations appropriate to "ices" (a mixture of CH_4, NH_3, and H_2O) and "rocks" (Fe, Ni, MgO and SiO_2), as described by Hubbard & Marley (1989).

Figure 1 compares different pressure-temperature profiles for Jupiter and Saturn, using the various equations of state described here. The figure is intended to provide an estimate of the uncertainties on the various equations of state (hydrogen-helium, heavy elements). It is important to notice at this point that Saturn's interior lies mostly in a relatively well-known region of the hydrogen-helium EOS, i.e. in which hydrogen is molecular, whereas a significant fraction of Jupiter's interior is at intermediate pressures (one to a few Mbar) for which the EOS is most uncertain.

2.5 Opacities

Although most of the interiors of Jupiter and Saturn are convectively unstable, some regions have been recognized to be potentially *stable*. At temperatures of the order of 1500 to 2000 K, a minimum of the Rosseland mean opacity (see, e.g., Clayton 1968 for a definition) is responsible for the likely presence of a radiative region in Jupiter, and perhaps Saturn (Guillot et al. 1994a). Much closer to the visible part of the atmospheres of these planets, the underabundance of some compounds, in particular water, may yield stable regions as well (see Guillot et al. 1994a; Fig.5). Those may however not cover the entire surface of the planet at a given level. Instead, 2- and 3-dimensional effects are to be expected due to meteorological phenomena.

The presence of radiative regions has major consequences on both static and evolution models of the giant planets: it yields significantly cooler interiors (Guillot et al. 1994b), and quickens their evolution (Guillot et al. 1995). It is therefore of prime importance to calculate accurate radiative opacities. In this work, I use a simplified opacity calculation, using the method described in Guillot et al. (1994a), and updated absorption data for water, methane, H_2S (see Marley et al. 1996 and references therein). The results of these preliminary calculations are presented in Table II, for a 3 times solar mixture. They are however much improved compared to previous calculations (Guillot et al. 1994a): as expected, including hot bands of water increased the opacity by as much as a factor 3 in some places, thereby significantly diminishing the extent and consequences of Jupiter's and Saturn's inner radiative zones. In the case of Saturn, the present models show no radiative zone, or a very limited one. The detailed study of the new absorption data on the presence and magnitude of the radiative zone will however have to await a more detailed calculation of an extended Rosseland opacity table (Freedman, personal communication 1999).

3 The three-layer structure assumption

Jupiter and Saturn are thought to be fluid and mostly convective (e.g., Hubbard 1968, Stevenson & Salpeter 1977, Guillot et al. 1994a), a consequence of their significant intrinsic heat flux (Hanel

Table II: Rosseland opacities (Logκ_{R}, in $\mathrm{g\,cm^{-2}}$)

	LogP (bar)				
LogT (K)	0.0	1.0	2.0	3.0	4.0
2.2	-1.68	-0.88	0.08	1.05	2.04
2.4	-1.75	-1.10	-0.29	0.50	1.32
2.6	-1.19	-0.58	-0.24	0.13	0.79
2.8	-1.08	-0.57	-0.30	0.09	0.81
3.0	-1.26	-0.89	-0.50	0.06	0.77
3.2	-2.17	-2.01	-1.68	-1.36	-0.85
3.4	-1.93	-1.83	-1.66	-1.34	-0.53
3.6	-1.02	-0.87	-0.72	-0.55	0.06

et al. 1981, 1983). It is natural to infer that their interiors should be homogeneously mixed, except where physical barriers prevent this mixing. It is thus commonly accepted that these planets should consist of a central core, a surrounding envelope in which hydrogen is metallic, and an overlaying molecular envelope which would have a chemical composition similar to what can be observed from the Earth (or rather, from deep probes). The division between each region is, in reality, rather vague. Figure 2 sketches the present perception of the interiors of Jupiter and Saturn. The following discussion aims at a careful examination of the three-layer assumption, and its limits.

3.1 The molecular envelope

The molecular envelope is the region that extends from the "surface" (since there is no gas/liquid or gas/solid phase transition, this usually refers to the visible troposphere, e.g., the 1 bar level), down to the level where hydrogen, instead of being molecular, becomes metallic. It is assumed to be quasi-homogeneous, and quasi-adiabatic, as discussed below.

With a pressure varying by more than six orders of magnitude from top to bottom, the molecular region is necessarily complex, thus casting some doubts on the assumption that it should be homogeneous. This is best exemplified by Jupiter's visible atmosphere. Due to condensation processes, the abundance of condensible species (NH_3, H_2O) varies both vertically and horizontally (Niemann et al. 1998; Roos-Serote et al. 1998). Similarly, complex chemical reactions occur (Fegley & Lodders 1994). However, since we are only interested in those chemical species that contribute significantly to the total fluid density (i.e., H_2O, essentially) these variations are expected to be confined to the upper part of the envelope and to have only small consequences on the calculated gravitational moments. They were however included in the present work, the effect being mimicked by using the saturation vapor pressure for water. The presence of refractory materials condensing at deeper levels was neglected, as their abundances are significantly smaller.

Condensation also tends to modify the temperature gradient, due to the latent heat released by condensing particles. Although the Galileo probe *in situ* measurements indicate that Jupiter's temperature profile is consistent with a dry adiabat, it is not clear that this is still valid out of the hot spot region (e.g., Showman & Ingersoll 1998). In fact, radio occultation data for Uranus and Neptune show that significant departures from a dry adiabat (generally steeper temperature profiles) occur in the region of methane condensation, and can amount to variations of the order of 5-10 K (Lindal 1992). This is interpreted as a consequence of the inhibiting action of molecular weight layering on convection (Guillot 1995). Latent heat release and molecular weight layering acting in opposite directions, it is not possible to tell whether the interiors of Jupiter and Saturn might be warmer or cooler than calculated assuming dry adiabatic profile. However, since they are expected to contain a much lower proportion of heavy elements than Uranus and Neptune, the changes on the temperature profile should not be as pronounced. Finally, it is noteworthy that upper regions in which the abundance of water is small, as was measured by the Galileo probe (Niemann et al. 1998), might be convectively stable (Guillot et al. 1994a, Seiff et al. 1998), which could also affect the temperature gradient. In summary, the temperatures in the 10-100 bar region and below appear to be more uncertain than those measured at 1 bar, but I regard the chosen 5 to 10 K uncertainty on the 1 bar temperature adequate as an estimate of the variations due to the temperature.

Opacity calculations predict the presence of a radiative region in Jupiter, at pressures between about 1.5 and 6 kbar, and temperatures between 1450 and 1900 K, and a tiny one, if any in Saturn. The presence of such a radiative region supposedly only affects the temperature profile, not the chemical composition. This is because any enrichment in heavy elements near the surface would be rapidly transported by downwelling "salt finger"-type plumes. Furthermore, evolution calculations (Guillot et al. 1995) show that this radiative zone, being essentially tied to the 1500-2000 K temperature level, moves inward in time, which has the tendency to smear any compositional gradient away. Finally, it is estimated that meridional circulation and differential rotation should allow further mixing of the elements in the radiative region.

In summary, the molecular envelopes of Jupiter and Saturn are supposed to be (dry) adiabatic, except where radiative opacities are low enough, and homogeneous. This means that, except for species that condense, the composition of the atmosphere is expected to be relevant to that of the entire molecular envelope. In particular, this is true of helium, whose measured mass mixing ratios in Jupiter and Saturn are smaller than inferred in the protosolar nebula. Helium is therefore believed to be hidden deeper, in the metallic region.

3.2 The metallic envelope

The distinction between the molecular and the metallic region is difficult to make, except in the presence of the PPT which then would have two physical effects: it would create an effective entropy barrier which wouldn't be crossed by convection (Stevenson & Salpeter 1977). It would also induce a discontinuity of the chemical composition, a consequence of the equality of the chemical potentials of the two phases (see Landau & Lifchitz 1984; Hubbard 1989). The molecular and metallic regions would then be relatively sharply separated, thus validating the present three-layer approach. The relative depletion of helium in the molecular regions of Jupiter and Saturn could then also be due to this chemical abundance discontinuity at the PPT, although this is generally not the preferred explanation because helium is expected to be more soluble in molecular than in metallic hydrogen (Stevenson & Salpeter 1977).

In the absence of a PPT, the presence of a hydrogen/helium phase *separation* becomes the only viable explanation for the low atmospheric Y in Jupiter and Saturn. Even if the PPT exists, a phase separation is likely to occur, both in Jupiter and Saturn, although it is expected that it is on larger scales inside Saturn because the planet is colder, has less helium in its atmosphere, and because homogeneous evolution models predict present day intrinsic heat flux much smaller than observed. In that case, it is estimated that helium-rich droplets would form, and grow rapidly, so that they would fall towards the interior without being efficiently transported by convection (Stevenson & Salpeter 1977). Furthermore, this phase separation is expected to lie close to the molecular/metallic transition (e.g., Stevenson 1982). In this work, I choose to assume that it occurs in a narrow region too, so that the helium-rich region is essentially the metallic part of the envelope. Consequently, I assume that, like the molecular region, the metallic one is homogeneous and adiabatic. The temperature and pressure are continuous across the transition, but not necessarily the chemical abundances, density and entropy.

In reality, hydrogen/helium separation may occur over a relatively wide range of pressure. Figure 2 shows that in the Mbar range, a relatively modest pressure variation from the helium poor to the helium rich regions can involve a non-negligible fraction of the planetary interior. It might even concern most of the metallic region if the slope of the critical line is as predicted by Pfaffenzeller et al. (1995) (see Guillot et al. 1995). Furthermore, even in the case of a shallow inhomogeneous region (with a gradient of helium concentration), a steep temperature gradient, which would be treated as a discontinuity of the temperature under the present assumptions, is to be expected. This jump should be relatively small however, according to the estimates by Stevenson & Salpeter (1977). Moreover, the density of metallic hydrogen is only weakly dependent on the temperature, and it can hence be neglected.

In summary, both major assumptions about the interior, i.e. that it is adiabatic and homogeneous, could be wrong in a (significant) part of the metallic region. Even in that somewhat least favorable case, the three-layer models are not expected to be fully irrelevant because the gravitational moments only probe extended regions of the interior (e.g., Zharkov & Trubitsyn 1974), and without other information such as measurements of oscillations, only constraints on averaged quantities can be sought from interior models.

3.3 The core

As we shall see, it is possible (although improbable) that Jupiter and Saturn have no cores. If present, the core has either been a seed on which the giant planets have grown (Lissauer 1993), or it has been formed early at the center of a very tenuous, non-convective protoplanetary clump (Boss 1998). Its composition is unknown, and cannot be inferred from the measurements of the gravitational moments (Guillot et al. 1994b). I somewhat arbitrarily assume that it is formed of a central mixture of rocks surrounded by ices, the ice to rock ratio being variable. I also assume that the transition between the core and the envelope is abrupt, although it might not be the case, depending on what happened during the formation period (Stevenson 1985). If layering occurs in the central regions, an intermediate inhomogeneous conductive region will link the core to the metallic region. It is unclear whether, in the framework of our three-layer model, the heavy elements present in such a region would be mostly included in the metallic region, or as core mass. In any case, the core masses given in this article are to be interpreted as masses of heavy elements located at or near the planetary center.

4 Construction of models

Interior models of the giant planets are calculated with the same set of equations that govern the structure and evolution of stars, with the exception that no thermonuclear reactions occur:

$$\begin{aligned}
\frac{\partial P}{\partial M} &= -\frac{GM}{4\pi R^4}+\frac{\omega^2}{6\pi R}+\frac{GM_{\rm tot}}{4\pi R_{\rm tot}^3 R}\varphi_\omega, &(5)\\
\frac{\partial T}{\partial M} &= \left(\frac{\partial P}{\partial M}\right)\frac{T}{P}\nabla_T, &(6)\\
\frac{\partial R}{\partial M} &= \frac{1}{4\pi R^2\rho}, &(7)\\
\frac{\partial L}{\partial M} &= -T\frac{\partial S}{\partial t}, &(8)
\end{aligned}$$

where the variables are: M, mass; R, mean radius; $M_{\rm tot}$, $R_{\rm tot}$: mass and radius at the "surface"; t, time; P, pressure; T, temperature; ρ, density; L, intrinsic luminosity; S, specific entropy; G, gravitational constant; $\nabla_T = \partial\log T/\partial\log P$, temperature gradient; ω is the angular velocity and φ_ω is a slowly varying function of the radius due to the high order centrifugal potential calculated within the theory of figures (Zharkov & Trubitsyn, 1978). In the case of static models (i.e. trying to reproduce the giant planets as we can observe them today rather than their entire evolution), Eq.(8) is not calculated. Instead, the intrinsic luminosity is fixed to its observed value, an approximation which is entirely justified, even in the presence of a radiative window (see Guillot et al. 1994b, 1995).

Solving this set of equations requires, apart from the usual boundary conditions (nullity of the luminosity at the center, and observed temperature at a given pressure level), the knowledge of:
(i) *the equation of state* $\rho(P,T,\{x_i\})$, where x_i denotes the fractional abundance of constituent i. In this work, I use the hydrogen-helium EOS from Saumon et al. (1995) in the molecular and metallic parts of the envelope, with the assumption that heavy elements can be embedded into an equivalent helium mass fraction which then accounts for their presence.
(ii) *the temperature gradient* ∇_T. It is determined by solving the radiative/convective equilibrium using the mixing length theory (e.g., Kippenhahn & Weigert 1991). In most of the interior, it is essentially equal to the adiabatic gradient obtained from the EOS: $\nabla_{\rm ad}\equiv(\partial\ln T/\partial\ln P)_S$.
(iii) *the chemical composition.* Within the adopted assumptions, the composition of the envelope is determined by only two quantities, $Y_Z^{\rm mol}$ and $Y_Z^{\rm met}$, the equivalent helium mass mixing ratio in the molecular and metallic regions, respectively. The composition of the core, of mass $M_{\rm core}$, is determined by the mass fraction of ices $f_{\rm ice}$, the rest being rocks.

The total mass of the planet being fixed, the observational constraints are the equatorial radius $R_{\rm eq}$ and gravitational moments J_2, J_4 and J_6, measured with respective observational uncertainties $\sigma_{R_{\rm eq}}$, σ_{J_2}, σ_{J_4} and σ_{J_6}. In the framework of the three-layer models, the adjustable parameters are $Y_Z^{\rm mol}$, $\Delta Y_Z\equiv Y_Z^{\rm met}-Y_Z^{\rm mol}$ and $M_{\rm core}$. A way of finding models matching the observational constraints is therefore to minimize the following function:

$$\chi^2(Y_Z^{\rm mol},\Delta Y_Z,M_{\rm core})=\frac{1}{4}\left[\left(\frac{\Delta R_{\rm eq}}{\sigma_{R_{\rm eq}}}\right)^2+\left(\frac{\Delta J_2}{\sigma_{J_2}}\right)^2+\left(\frac{\Delta J_4}{\sigma_{J_4}}\right)^2+\left(\frac{\Delta J_6}{\sigma_{J_6}}\right)^2\right], \tag{9}$$

where $\Delta R_{\rm eq}$, ΔJ_2, ΔJ_4, ΔJ_6 are the differences between observed and theoretical $R_{\rm eq}$, J_2, J_4 and J_6. For a given ΔX, not too large in absolute value, it is generally possible to find a well-defined, very sharp minimum of χ^2 (Figs. 3, 4). In fact, the minimum is so sharp that the solution ($M_{\rm core}$, $Y_Z^{\rm mol}$) can be thought of as being unique, i.e. leading to an accurately defined value of J_4. The choice of a different ΔY_Z induces a different solution ($M_{\rm core}$, $Y_Z^{\rm mol}$), and a different final value of J_4. The non-uniqueness of solutions matching the observed gravitational fields is therefore mostly due the uncertainty of J_4. So far, no useful constraint can be derived from the values of J_6, owing to their large observational uncertainties (see Table I).

For each model solution, it is then possible to retrieve the mass fraction of heavy elements in the molecular and metallic parts of the envelope. This is done by using the observed helium mass fraction in the molecular envelope $Y^{\rm mol}$ and by retrieving that in the metallic envelope $Y^{\rm met}$ by using the fact that the total helium to hydrogen ratio should be equal to its value in the protosolar nebula. The value of Z at each level is then obtained by the following relation:

$$Z = (Y_Z - Y)\frac{\rho_{\rm H}^{-1} - \rho_{\rm He}^{-1}}{\rho_{\rm H}^{-1} - \rho_{\rm Z}^{-1}}, \tag{10}$$

where $\rho_{\rm H}$, $\rho_{\rm He}$ and $\rho_{\rm Z}$ are the densities of pure hydrogen, pure helium and heavy elements, respectively. As described by Guillot et al. (1997), Eq. 10 does not ensure that Z is constant, even in regions where Y_Z and Y are. These departures having no physical meaning, $Z^{\rm mol}$ and $Z^{\rm met}$ are estimated by averaging Eq. 10 over the molecular and metallic regions, respectively.

Finally, in order to obtain meaningful constraints on the internal composition of the giant planets, the following uncertainties have to be taken into account:

On the equations of state: two EOSs from Saumon et al. (1995) are used for the hydrogen-helium mixture. Because they are both qualitatively and quantitatively very different from one another, their use should provide a relatively good estimate of the uncertainties that are to be expected on the behavior of these elements at high pressures. On the other hand, the EOS for heavy elements is even more uncertain because both their composition and high pressure behavior are mostly unknown. The estimated uncertainties on ρ_Z (that enters Eq. 10) are shown in Fig. 1 (see Guillot et al. 1997 for a more detailed description).

On the temperature profile: the interior was either assumed to be fully adiabatic, or calculated by consistently solving for the radiative/convective equilibrium, thus allowing for a radiative region to appear.

On the internal rotation: Hubbard (1982) has shown that the presence of differential rotation can lead to a significant change in the calculated gravitational moments. This change is, in terms of observational error, most important for the lower order moments. In fact, the effect on J_2 leads only to a negligible modification of the values of $Y_Z^{\rm mol}$, ΔY_Z and $M_{\rm core}$ that reproduce the observed J_{2i}. However, the modification of J_4 by differential rotation is very significant, as shown hereafter.

5 Results

5.1 Sensitivity to changes of the density profiles

As discussed previously, the density profile in the planetary interior can vary, due to several causes (equation of state, temperature, composition). However, only the density profile itself is constrained by the gravitational field measurements. It is therefore useful to estimate the effect of a change of the density profile on the various parameters and results of the optimization procedure.

In order to do so, two reference models are calculated for Jupiter and Saturn. Comparison models are then computed, with a slightly different EOS: instead of a density $\rho_0(P,T)$, I use $\rho(P,T)$, which has been arbitrarily increased compared to ρ_0 by 5% at P_0, using the following relation:

$$\rho(P,T) = \rho_0(P,T)\left[1 + 0.05e^{-\log^2(P/P_0)}\right], \tag{11}$$

The comparison models are optimized by varying $Y_Z^{\rm mol}$ and $M_{\rm core}$ so that $R_{\rm eq}$ and J_2 are always equal to their observed value (of course, the total mass of the planet is held constant!). The variations of J_4 that result are shown by a dotted line on Fig. 5. They can amount to up to 2σ for Jupiter and 0.5σ for Saturn (but the uncertainty on the measured value of J_4 is larger). For example, a model of Jupiter which at first fitted the observed gravitational moments gets its J_4 shifted by 2σ after a 5% increase of the density in the 10 Mbar region.

The additional constraint that J_4 should also remain fixed requires an additional free parameter: ΔY_Z. A unique solution ($M_{\rm core}$, $Y_Z^{\rm mol}$, $Y_Z^{\rm met}$) can then be sought. Its changes as a function of P_0 are shown in Fig. 5. In both Jupiter and Saturn, up to $2\,M_\oplus$ variations of the core masses are observed in consequence to a localized 5% density change. Note, however, that a 5% density change everywhere (i.e. independant of P) would only scarcely affect the core mass, as can be seen by integrating over $\log P$ the plain curve in Fig. 5. Jupiter and Saturn react differently to a density change at pressure P_0: inside Jupiter, a density change at pressures lower than 0.1 Mbar involves only the outermost 5% (in radius) of the planet and is therefore barely seen. In Saturn, this corresponds to more than 11% of the planet. Furthermore, the molecular/metallic transition is at 80% of the planetary radius in Jupiter, and about 50% in Saturn. The consequence is that, in terms of gravitational moments, Saturn's metallic region is essentially indistinguishable from a large core. This is also seen from the large variations of $Y_Z^{\rm met}$ with P_0 for this planet.

5.2 Constraints from the gravity field

The constraints obtained solely from the static models are shown by the dashed regions of Fig. 6 and 7. As expected, the uncertainties on the hydrogen-helium EOS are much more apparent in Jupiter than in Saturn, especially when one considers the core masses and total masses of heavy elements obtained. In Jupiter, the solutions obtained with the *i*-EOS and with the PPT-EOS do not overlap. I however consider that all the solutions inbetween are acceptable, as these two EOSs are characteristic of the uncertainties of the high-pressure EOSs in general. In the case of Saturn, the PPT-EOS yields generally smaller quantites of heavy elements, mostly in the metallic region, but the difference with the *i*-EOS is of the order of $3\,M_\oplus$ only.

As shown in Fig. 6, the core masses obtained are $0-14\,M_\oplus$ for Jupiter and $0-22\,M_\oplus$ for Saturn. The total masses of heavy elements in these planets are $11-42\,M_\oplus$ and $19-31\,M_\oplus$, respectively. Unfortunately, it is not possible to tell from this work which of Jupiter or Saturn contains the largest amount of heavy elements, a fundamental question in the quest of their origin.

If the total amount of heavy elements is poorly constrained in Jupiter, and rather well constrained in Saturn, the reverse is almost true when considering the detailed enrichment in the molecular and metallic envelopes, as seen on Fig. 7. As a result, $Z^{\rm mol}$ is between 0.7 and 6.5 times solar, and $Z^{\rm met}$ is between 0 and 7 times solar in Jupiter. The situation is slightly more complex in Saturn, because of the uncertainty on the mass mixing ratio of helium in the atmosphere. The constraints resulting from the use of the Voyager helium mass mixing ratios ($Y = 0.06 \pm 0.05$), shown as a horizontally-dashed area, are, in solar units, $4.5 < Z^{\rm mol} < 13$ and $0 < Z^{\rm met} < 25$. However, for reasons that will be explained in the next section, a larger value of $Y^{\rm mol}$ is probably more realistic. The ensemble of solutions for $Y^{\rm mol} = 0.16 \pm 0.05$, 2σ away from the Voyager value, is $2 < Z^{\rm mol} < 10.5$. This value is thus in better agreement with the abundance of methane derived from spectroscopic data. Unfortunately, no useful constraint on $Z_{\rm met}$ can be inferred from these models.

The results of Fig. 6 agree fairly well with interior models calculated within the last ten years: Hubbard & Marley (1989) allowed the density profile to vary in the molecular/metallic hydrogen transition region and found that the more regular solutions had cores of the order of 8 to 12 $\rm M_\oplus$ for Jupiter, and 9 to 20 $\rm M_\oplus$ for Saturn. The total masses of heavy elements that can be inferred from that work is about 30 $\rm M_\oplus$ and $20-30$ $\rm M_\oplus$ for Jupiter and Saturn, respectively. Zharkov & Gudkova (1992), using five layers models, and a different, fixed equation of state, found rock/ice core masses of about 5 $\rm M_\oplus$ for Jupiter and 7 $\rm M_\oplus$ for Saturn, these planets containing about 50 $\rm M_\oplus$ and 25 $\rm M_\oplus$ of heavy elements, respectively. Finally, Chabrier et al. (1992), with the same equations of state as used by Guillot et al. (1994) and Guillot, Gautier & Hubbard (1997), found core masses of 4 to 8 $\rm M_\oplus$ and 1 to 20 $\rm M_\oplus$, and total masses of heavy elements of 10 to 16 $\rm M_\oplus$ and 24 to 30 $\rm M_\oplus$ for Jupiter and Saturn, respectively.

Generally larger core masses (10-30 $\rm M_\oplus$) were found in previous calculations (see Stevenson 1982 for a review), but the largest core masses also yielded helium mass fractions well below the protosolar value that were therefore unrealistic. The main reason for the discrepancy with today's values is however that the calculation of core masses is, especially in the case of Jupiter, very sensitive to changes in the equation of state, and that the core masses have decreased as the equation of state of hydrogen has improved.

Table III: Constraints on ΔY_Z from static interior models

	i-EOS	PPT-EOS
Jupiter adiabatic 165K	0.013 to 0.060	−0.051 to 0.039
170K	0.003 to 0.060	−0.061 to 0.029
radiative 165K	0.029 to 0.078	−0.030 to 0.061
170K	0.003 to 0.078	−0.033 to 0.057
Saturn adiabatic 135K	0.29 to 0.55	0.21 to 0.57
145K	0.09 to 0.46	0.003 to 0.46

An important parameter derived from these static models matching the observed gravitational moments is the discontinuity of the equivalent mass mixing ratio of helium ΔY_Z, as it can be linked to results obtained from evolution models. The constraints interior models provide to this parameter are given in Table III.

Finally, the relative importance of the various sources of uncertainties included in this work on the solutions are indicated by arrows in Figs. 6 and 7. One of the most significant sources of uncertainty, apart from that relative to the various equations of state, is that on the gravitational moment J_4. A 1σ change of this variable would amount to variations of $M_{\rm core}$ by $\sim 3\,\rm M_\oplus$ in Jupiter, and by $\sim 10\,\rm M_\oplus$ in Saturn, and to large variations of of $Z^{\rm met}$ and $Z^{\rm mol}$. A much better determination of that parameter by future missions (including, most importantly, the Cassini-Huygens mission at Saturn) will therefore help to considerably reduce the uncertainties on the model solutions. Unfortunately, the presently unknown interior rotation field will set a limit on the improvements that can be expected from such a determination, as shown by the arrows labeled Ω in Figs. 6 and 7. A better determination of the opacities will also be a task to work on in order to gain precision in the models.

In the case of Saturn, significant improvements are to be expected from measurements by the Cassini-Huygens mission since the uncertainties associated with the equations of state are relatively small for that planet. For example, a carefully determined 1 bar temperature will help to improve constraints on the core mass, $Z^{\rm mol}$ and $Z^{\rm met}$. A higher surface temperature (145K instead of 135K) would thus yield a $\sim 4\,{\rm M}_\oplus$ larger $M_{\rm core}$, values of $Z^{\rm mol}$ larger by 1.8 solar values, and of $Z^{\rm met}$ smaller by 7 solar values. Furthermore, a better defined surface helium mass mixing ratio $Y^{\rm mol}$ is highly desirable, as a 1σ variation (with the current observational uncertainty) yields an uncertainty on $Z^{\rm mol}$ which amounts to ~ 2 times the solar value.

5.3 Consistency with evolution models

Table IV: Ages derived from homogeneous evolution models (in Gyr)

	i-EOS	PPT-EOS
Jupiter adiabatic	4.7	5.1
radiative	3.6	4.5
Saturn adiabatic	2.0	2.7
radiative	2.0	2.2

In this section, better constraints are sought from evolution models, which are described in detail in the companion paper by Hubbard et al. (1999). Model ages assuming *homogeneous* evolutions (see Guillot et al. 1995), and corrected for the variable solar luminosity are given in Table IV. Compared to the age of the Solar System, 4.55 Gyr, Jupiter and Saturn formed on a relatively short time scale, at most 0.02 Gyr (e.g., Pollack et al. 1996). Any difference between the ages in Table IV and that of the Solar System has therefore to be explained by either uncertainties inherent to the evolution calculations (probably less than 0.3 Gyr), or by physical phenomena, among which differentiation appears to be the most likely. The time delay due to helium differentiation can be estimated by the following relation (see Hubbard et al. 1999):

$$\Delta t \simeq \begin{cases} 9.1\,\Delta Y & \text{for Jupiter,} \\ 8.3\,\Delta Y & \text{for Saturn,} \end{cases} \tag{12}$$

where Δt is in Gyr, and ΔY could represent the differentiation of either helium or any other elements (e.g., water, if it is abundant enough). One can see that a negative ΔY would yield a faster evolution, as heavy elements are then transported upward against gravity, thereby consuming some of the internal luminosity. However, this situation is extremely unlikely, as this would mean that helium differentiation would be more than balanced by that of other elements, which *a priori* are less abundant. I therefore assume that ΔY is positive. Some of the models of Table IV, in particular the adiabatic PPT-EOS Jupiter evolution models, are thus incompatible with the age of the Solar System.

Eq. 12 assumes that ΔY is a linearly increasing function of time. This assumption fails in two cases: (i) if the planet was initially formed with this abundance discontinuity or (ii) if most of the evolution from homogeneity to the present ΔY occurred early, as might happen with a compositional discontinuity caused by the PPT. Eq. 12 might hence overestimate somewhat the time delay Δt, in which case larger ΔY (or equivalently ΔY_Z) would then be possible. I choose however, not to account for this possibility. The age constraints ΔY_Z are derived directly from Eq. 12, the difference between the ages in Table IV and that of the Solar System, assuming an uncertainty of ±0.3 Gyr for Jupiter and ±0.5 Gyr for Saturn.

Table V: Constraints on ΔY_Z from evolution models

	i-EOS	PPT-EOS
Jupiter adiabatic	$-0.05^\star$ to 0.01	$-0.10^\star$ to $-0.03^\star$
radiative	0.06 to 0.13	$-0.03^\star$ to 0.03
Saturn adiabatic	0.24 to 0.36	0.15 to 0.28
radiative	0.24 to 0.36	0.21 to 0.34

*: Negative values of ΔY_Z are unlikely (see text).

The constraints thus obtained are summarized in Table V. They can be compared to the previous ones (Table III), the intersection of the two providing a tighter global constraint. It is obvious, in the case of Saturn, that significant helium differentiation is required to provide the planet enough energy so as to slow its cooling by about 2 Gyr or more. However, large ΔY_Z such as those predicted in the case of models with no cores would provide too much energy, unless most of the differentiation occurred early in the evolution, as discussed below.

An interesting side result can be derived with the additional assumption that negligible differentiation of heavy elements occurs between the molecular and the metallic regions, except any compositional discontinuity that would occur during the formation epoch, and would thus not affect Eq. 12. This assumption is realistic, as helium is, due to its large abundance, the element which is the most likely to separate from hydrogen (see, e.g., the critical temperatures and abundances derived by Brami et al. 1979, in the fully ionized regime). It is however not proven, and therefore needs to be confirmed by experiments, or detailed theoretical calculations.

With that assumption, the external helium abundance $Y^{\rm mol}$ can then be derived. I write the constraint on the conservation of the total quantity of helium:

$$Y^{\rm mol} = Y_{\rm proto} - \frac{m_{\rm t} - m_{\rm c}}{1 - m_{\rm c}} \Delta Y, \tag{13}$$

in which $Y_{\rm proto}$ is the protosolar helium mass mixing ratio, $m_{\rm c}$ the adimensional core mass and $m_{\rm t}$ the mass at the molecular/metallic transition. I choose $m_{\rm t} \sim 0.85$, $m_{\rm c} \sim 0$ for Jupiter and $m_{\rm t} \sim 0.5$, $m_{\rm c} \sim 0.1$ for Saturn. Table VI is then derived from Eq. 13 and the constraints from Tables III and V. It shows that *radiative* models of Jupiter globally agree with the observed helium mass mixing ratio, $Y = 0.238$, although this probably requires an EOS intermediate between the i-EOS and the PPT-EOS. On the other hand, they would not have agreed (or only marginally) with the previous value $Y = 0.18 \pm 0.04$. Similarly, the values derived for Saturn, between 0.11 and 0.21, disagree with the Voyager value $Y = 0.06 \pm 0.05$. If helium separation occurs deeper in the planet, the problem becomes even more acute: for example, with $m_t = 0.3$, I derive $Y^{\rm mol} = 0.19$ to 0.25. Similarly, if any other element separates from hydrogen as well, the additional energy would require still larger values of $Y^{\rm mol}$. A higher value of the surface (molecular) helium mass mixing ratio is therefore required, a problem that will certainly be addressed by the Cassini-Huygens mission.

Table VI: Derivation of the values of $Y^{\rm mol}$

	i-EOS	PPT-EOS
Jupiter adiabatic	0.26 to 0.28	—
radiative	0.20 to 0.23	0.24 to 0.28
Saturn adiabatic	0.11 to 0.17	0.14 to 0.21
radiative	0.11 to 0.17	0.12 to 0.18

In Figs. 6 and 7, the constraints derived from evolution models are represented by shaded regions. They are clearly smaller than those derived from static models only. In the case of Jupiter, two separated regions represent the solutions for the two EOSs used here. Clearly, a better-defined EOS is needed. The core mass is thus constrained to lie between 0 and 10 Earth masses, but the constraints on the total mass of heavy elements are not improved. The new constraints also indicate that Jupiter's molecular envelope is enriched in heavy elements by a factor 1.5 to 6.5 compared to the solar value, and its metallic envelope by at most a factor ~ 6.5 (Fig. 7).

On the contrary, significantly tighter constraints are obtained from evolution models in the case of Saturn. A lower core mass limit of $6\,{\rm M}_\oplus$ can be inferred. Models with smaller cores require abundance discontinuities ΔY_Z that would yield ages larger than that of the solar system. This constraint is however less robust than that derived from the gravitational moments only, as it could be invalidated by an early differentiation that would not obey Eq. 12. This is however unlikely, as it is difficult to understand why such an early differentiation would not have occurred in Jupiter as well. The upper core mass limit is 16 ${\rm M}_\oplus$. Saturn's core mass therefore appears to be larger than that of Jupiter, but this could be an artifact due, first to the rather large error bars, and second to the fact that helium differentiation may yield an extended inhomogeneous region in Saturn's metallic region.

In Saturn, the case for a higher atmospheric helium mixing ratio than inferred from Voyager is further strengthened by a derivation of $Z^{\rm mol}$, shown in Fig. 8. A value $Y^{\rm mol}$ less than 0.11 (the upper limit of the Voyager value obtained by Conrath et al. 1984) yields enrichments in heavy elements larger than 6.5 times the solar value, which is extremely difficult to reconcile with the observed abundance of methane in that atmosphere. The problem is of course complicated by the condensation of many species to deeper levels, in particular water, and the consequent impossibility to determine their abundances. However, it seems difficult to imagine that the C/O ratio would be extremely different from solar. On the contrary, higher values of $Y^{\rm mol}$ yield enrichments that agree with spectroscopic measurements of Saturn's atmosphere. It is noteworthy that a high $Y^{\rm mol}$ value necessitates that Saturn's metallic envelope be richer in heavy elements than its molecular envelope. This presumably would indicate the absence of a global mixing of the planetary interior throughout its evolution, the inner regions, which formed early, having been impacted by many more planetesimals in the early protoplanetary phases than the final planet itself.

5.4 The values of J_4 and J_6

An interesting side result concerns the values of J_4 and J_6 obtained assuming solid rotation (only the *measured* observational moments have been adjusted for differential rotation), shown in Fig. 9. The values of J_4 were constrained to be within the observational error bars, but it can be seen that, both in the case of Jupiter and Saturn, the models with the additional evolution constraint (large symbols) are generally in better agreement with a solid internal rotation than with a surface differential rotation extending deep in the interior (Hubbard 1982). The uncertainties on the measurements are however still too large to be conclusive. Again, more accurate J_4 measurements may resolve the issue of the presence of a core, as models with no core always possess smaller $|J_4|$.

From Jupiter to Saturn, a close proportionality relation links J_6 to J_4, almost independently of any assumed uncertainty (on the equation of state, temperature profile, condensation of heavy elements...etc.). This is not unexpected, as the uncertainties on the density profile in the external layers are rather small, and these profiles are continuous. The theoretical values for J_6 are between 0.35 and 0.38×10^{-4} for Jupiter, and between 0.9 and 0.98×10^{-4} for Saturn. These values are thus defined with a precision which is about 10 times larger than the current observational uncertainties. Should measurements point to different values of J_6, major changes in interior models would have to be found, probably invoking significant departures from the three-layer assumption, and/or very peculiar differential rotation patterns. For example, an abstract by Bosh (1994) states that a more accurate value of J_6 can be obtained for Saturn by constraints added by measurements of the position of non-circular ringlets of the planet. The thus inferred value (adjusted to the 1 bar equatorial radius given in Table I), $J_6 = 1.25 \pm 0.06 \times 10^{-4}$, is incompatible with all interior models presented here. This has also been verified by Gudkova & Zharkov (1997).

Measurements by the Cassini orbiter should provide accurate measurements of J_4 and J_6, and therefore test interior models. It also has been proposed that a Jupiter close orbiter would allow the precise determination of the planet's gravitational moments up to a relatively high order (~ 12), and would thus constrain the deep internal rotation (Hubbard 1999). Such a mission would also provide an excellent test of interior models of Jupiter.

5.5 The D/H ratios

The measurement of the deuterium to hydrogen isotopic ratio in the giant planets could be a powerful way to determine the abundance of ices in their interiors, as this isotopic ratio $(\mathrm{D/H})_{\mathrm{ices}}$ is, in the interstellar medium, higher in ices ($\mathrm{HDO/H_2O}$) than in hydrogen ($\mathrm{HD/H_2}$). The giant planets are expected to contain slightly more deuterium than the protosolar value $(\mathrm{D/H})_{\mathrm{proto}}$, in proportion to their enrichment in heavy elements (Hubbard and MacFarlane 1980; Lécluse et al. 1996):

$$(\mathrm{D/H}) = \frac{M_{\mathrm{H_2}}(\mathrm{D/H})_{\mathrm{proto}} + \frac{2}{18}M_{\mathrm{H_2O}}(\mathrm{D/H})_{\mathrm{H_2O}}}{M_{\mathrm{H_2}} + \frac{2}{18}M_{\mathrm{H_2O}}}, \tag{14}$$

where $M_{\mathrm{H_2}}$ and M_{H2O} are the masses of the hydrogen and water reservoirs, respectively, that were allowed to exchange their deuterium, and $(\mathrm{D/H})_{\mathrm{H_2O}}$ is the deuterium ratio in water whose assumed value, 300 ppm, is representative of that found in comets so far (Bockelée-Morvan et al. 1998). Other compounds may also have a small contribution to the deuterium enrichment but are neglected.

Figure 10 compares the D/H ratios measured on Jupiter (Mahaffy et al. 1998) and Saturn (Griffin et al., 1996) to the theoretical values estimated from the interior models matching both the gravitational and evolution constraints. Two theoretical calculations were performed for each planet, one for which the total amount of ices was allowed to exchange its deuterium with the hydrogen reservoir, another for which the core was kept separated from the envelope (i.e. material in the core never mixed with the hydrogen in the envelope, even during the formation of the planets). The mass of water (and other deuterium-carriers) that contributed to the heavy element content of the giant planets was supposed to lie between 1/2 and 2/3 of the total mass of heavy elements now present in these planets. As a result, even if Jupiter and Saturn have been enriched in deuterium by ices with relatively high D/H ratios, this enrichment is still too small to be detected, given the large observational error bars.

A better observational determination of the deuterium abundances in Jupiter and Saturn is to be sought. If measured with an accuracy of the order of 1ppm, a comparison of the values obtained for the two planets would allow an estimate of the deuterium content of the primordial ice carriers, thus testing the hypothesis that ices that formed planetesimals vaporized and had time to exchange their deuterium in the hot early protosolar nebula (Drouart et al. 1999).

6 Conclusions

Constraints on the internal structure and composition of Jupiter and Saturn have been derived within the framework of the three-layer model. For the first time, constraints from both the planets' gravitational fields and their evolution have been used. The uncertainties of the result are still large, mostly because of our limited knowledge of the behavior of hydrogen and of hydrogen/helium mixtures at pressures greater that 1 Mbar.

Yet interior models indicate that both Jupiter and Saturn are enriched in heavy elements compared to the Sun (or, equivalently, the protosolar nebula). How the planets acquired these additional heavy elements is still a mystery. Unfortunately, a comparison of core masses and amounts of heavy elements in Jupiter and Saturn is still inconclusive. Most importantly, it is not yet possible to decide which of Jupiter and Saturn possesses the largest absolute quantity of elements other than hydrogen and helium.

From this work, one cannot rule out either core accretion or gaseous instability as valid formation mechanisms for Jupiter. Uncertainties on the hydrogen equation of state greatly affect the accuracy of the results obtained for that planet, and both a low and a high heavy elements content (which, presumably would be incompatible with a rapid formation of the planet, as its capture radius would become small on time scales shorter than 1 Myr) are possible.

In the case of Saturn, constraints from the interior and evolution models, indicate that a significant fraction of the heavy elements lie in the dense core and in the metallic envelope. This is difficult to reconcile with the formation of this planet by gaseous instability.

Although, it will be difficult to accurately determine the structure of the interiors of Jupiter and Saturn in the foreseeable future, progress is to be expected from high pressure experiments on liquid hydrogen (or deuterium) and the corresponding theoretical improvements on the equation of state of that material, from better determinations of Saturn's helium abundance in its atmosphere, from measurements of the high order gravitational moments (beginning with J_4) in Jupiter and Saturn, and from theoretical improvements on opacity data and non-homogeneous evolution models including hydrogen/helium phase separation.

Acknowledgments

I wish to thank D. Gautier, W.B. Hubbard and D. Saumon for many helpful discussions and e-mail exchanges, and T. Owen for carefully reading this manuscript. This work was supported by the *Groupe de Recherche Structure Interne des Etoiles et des Planètes Géantes* and by the *Programme National de Planétologie*. It has been performed using the computing facilities provided by the program "Simulations Interactives et Visualisation en Astronomie et Mécanique (SIVAM)".

References

Anders, E., Grevesse, N. 1989. Abundances of the elements: meteoritic and solar. *Geochim. Cosmochim. Acta* **53**, 197–214.

Bahcall, J.N., Pinsonneault, M.H. 1995. Solar models with helium and heavy elements diffusion. *Rev. Mod. Phys.* **67**, 781–808.

Bockelée-Morvan, D., Gautier D., Lis, D.C., Young, K., Keene, J., Phillips, T., Owen, T., Crovisier, J., Goldsmith, P.F., Bergin, E.A., Despois, D., Wootten, A. 1998. Deuterated water in comet C/1996 B2 (Hyakutake) and its implications for the origin of comets. *Icarus* **133**, 147–162.

Bosh, A.S. 1994. Saturn's non-circular ringlets and gravitational harmonics. *Ann. Geophys.* **12**, C676 [abstract].

Boss, A. P. 1998. Evolution of the Solar Nebula IV - Giant Gaseous Protoplanet formation. *Astrophys. J.* **503**, 923–937.

Brami, B., Hansen, J-P., Joly, F. 1979. Phase separation of highly dissymmetric binary ionic mixtures. *Physica* **95A**, 505–525.

Burrows, A., Marley, M.S., Hubbard, W.B., Lunine, J.I., Guillot, T., Saumon, D., Freedman, R., Sudarsky, D. & Sharp, C. 1997. A nongray theory of extrasolar giant planets and brown dwarfs. *Astrophys. J.* **491**, 856–875.

Busse, F.H. 1976. A simple model of convection in the Jovian atmosphere. *Icarus* **29**, 255-260.a

Cameron, A.G.W. 1978. Physics of the primitive solar accretion disk. *Moon Plan.* **18**, 5–40.

Campbell, J.K., Synnott, S.P. 1985. Gravity field of the jovian system from Pioneer and Voyager tracking data. *Astron. J.* **90**, 364–372.

Campbell, J.K., Anderson, J.D. 1989. Gravity field of the saturnian system from Pioneer and Voyager tracking data. *Astron. J.* **97**, 1485–1495.

Carlson, B.E., Lacis, A. A., Rossow, W. B. 1992. The abundance and distribution of water vapor in the Jovian troposphere as inferred from Voyager Iris observations. *Astrophys. J.* **388**, 648-688.

Chabrier, G., Saumon, D., Hubbard, W.B., Lunine, J.I. 1992. The molecular-metallic transition of hydrogen and the structure of Jupiter and Saturn. *Astrophys. J.* **391**, 817–826.

Clayton, D.D. 1968. *Principles of stellar evolution and nucleosynthesis*, Univ. Chicago Press, Chicago (Revised edition: 1983).

Collins, G.W., Da Silva, L.B., Celliers, P., Gold, D.M., Foord, M.E., Wallace, R.J., Ng, A., Weber, S.V., Budil, K.S., Cauble, R. 1998. Measurements of the equation of state of deuterium at the fluid insulator-metal transition. *Science* **281**, 1179–1181.

Conrath, B.J., Gautier, D., Hanel, R., Lindal, G., Marten, A. 1984. The helium abundance of Saturn from Voyager measurements. *Astrophys. J.* **282**, 807-815.

Conrath, B.J., Hanel, R.A.,Samuelson, R.E. 1989. Thermal structure and heat balance of the outer planets. In *Origin and Evolution of Planetary and Satellite Atmospheres* (eds. S.K. Atreya, J.B. Pollack, and M.S. Matthews), Univ. of Arizona Press, Tucson, pp. 513–538.

Da Silva, L.B., Celliers, P., Collins, G.W., Budil, K.S., Holmes, N.C., Barbee, III, T.W., Hammel, B.A., Kilkenny, J.D., Wallace, R.J., Ross, M., Cauble, R. 1997. Absolute equation of state measurements on shocked liquid deuterium up to 200 GPa (2 Mbar). *Phys. Rev. Lett.* **78**, 483–486.

de Pater, I., Massie, S.T. 1985. Models of the millimeter-centimeter spectra of the giant planets. *Icarus* **62**, 143–171.

Drouart, A., Dubrulle. B., Gautier, D., Robert, F. 1999. Structure and transport in the solar nebula from constraints on deuterium enrichment and giant planets formation. *Icarus*, in press.

Fegley, B.Jr., Lodders, K. 1994. Chemical models of the deep atmospheres of Jupiter and Saturn. *Icarus* **110**, 117–154.

Folkner W.M., Woo, R., Nandi, S. 1998. Ammonia abundance in Jupiter's atmosphere derived from the attenuation of the Galileo probe's radio signal. *Journal Geophys. Res.* **103**, 22831–22846.

Gautier, D., Bézard, B., Marten, A., Baluteau, J.-P., Scott, N., Chedin, A., Kunde, V., Hanel, R. 1982. The C/H ratio in Jupiter from the Voyager infrared investigation. *Astrophys. J.* **257**, 901–912.

Gautier D., Owen, T. 1989. Composition of outer planet atmospheres. In *Origin and Evolution of Planetary and Satellite Atmospheres* (eds. S.K. Atreya, J.B. Pollack, and M.S. Matthews), University of Arizona Press, Tucson, pp. 487–512.

Geiss, J., Gloecker, G. 1998. Abundances of deuterium and helium-3 in the protosolar cloud. *Space Sci. Rev.* **84**, 239–250.

Gierasch, P.J., Conrath, B.J. 1993. Dynamics of the atmospheres of the outer planets - Post-Voyager measurement objectives. *J. Geophys. Res.* **98**, 5459-5469.

Griffin, M.J., Naylor, D.A., Davis, G.R., Ade, P.A.R., Oldham, P.G., Swinyard, B.M., Gautier, D., Lellouch, E., Orton, G.S., Encrenaz, T., De Graauw, T., Furniss, H., Smith, I., Armand, C., Burgdorf, M., Di Giorgio, A., Ewart, D., Gry, C., King, K.J., Lim, T., Molinari, S., Price, M., Sidher, S., Smith, A., Texier, D., Trams, N., Unger, S.J., and Salama, A. 1996. First detection of the 56-μm rotational line of HD in Saturn's atmosphere. *Astron. Astrophys.* **315**, L389-L392

Gudkova, T.V., Zharkov, V.N. 1997. Models of Jupiter and Saturn with water-depleted atmospheres. *Solar Sys. Res.* **31**, 99–107.

Guillot, T., Gautier, D., Chabrier, G., Mosser, B. 1994a. Are the giant planets fully convective? *Icarus*, **112**, 337–353.

Guillot, T., Chabrier, G., Morel, P., Gautier, D. 1994b. Non-adiabatic models of Jupiter and Saturn. *Icarus*, **112**, 354–367.

Guillot, T. 1995. Condensation of methane, ammonia and water and the inhibition of convection in giant planets. *Science* **269**, 1697–1699.

Guillot, T., Chabrier, G., Gautier, D., Morel, P. 1995. Radiative transport and the evolution of Jupiter and Saturn. *Astrophys. J.* **450**, 463–472.

Guillot, T., Gautier, D., Hubbard, W.B. 1997. New constraints on the composition of Jupiter from Galileo measurements and interior models. *Icarus* **130**, 534–539.

Hanel, R.A., Conrath, B.J., Herath, L.W., Kunde, V.G., Pirraglia, J.A. 1981. Albedo, internal heat, and energy balance of Jupiter: Preliminary results of the Voyager infrared investigation. *J. Geophys. Res.* **86**, 8705–8712.

Hanel, R.A., Conrath, B.J., Kunde, V.G., Pearl, J.C., Pirraglia, J.A. 1983. Albedo, internal heat flux, and energy balance of Saturn. *Icarus* **53**, 262–285.

Holmes, N.C., Ross, M., and Nellis, W.J. 1995. Temperature measurements and dissociation of shock-compressed liquid deuterium and hydrogen. *Phys. Rev. B* **52**, 15835–15845.

Hubbard, W.B. 1968. Thermal structure of Jupiter. *Astrophys. J.* **152**, 745–753.

Hubbard, W.B., MacFarlane, J.J. 1980. Theoretical predictions of deuterium abundances in the jovian planets. *Icarus* **44**, 676–682.

Hubbard, W.B. 1982. Effects of differential rotation on the gravitational figures of Jupiter and Saturn. *Icarus* **52**, 509–515.

Hubbard, W.B. 1989. Structure and composition of giant planets interiors. In *Origin and Evolution of Planetary and Satellite Atmospheres*, S. K. Atreya, J. B. Pollack, and M. S. Matthews, eds., University of Arizona Press, Tucson, pp. 539–563.

Hubbard, W.B., Marley, M.S. 1989. Optimized Jupiter, Saturn and Uranus interior models. *Icarus* **78**, 102–118.

Hubbard, W.B., Guillot, T., Lunine, J.I., Burrows, A., Saumon, D., Marley, M.S., Freedman, R.S. 1997. Liquid metallic hydrogen and the structure of brown dwarfs and giant planets, *Physics of Plasmas*, **4**, 2011–2015.

Hubbard, W.B. 1999. Gravitational signature of Jupiter's deep zonal flows. *Icarus* **137**, 196–199.

Hubbard, W.B., Guillot, T., Marley, M.S., Burrows, A., Lunine, J.I., Saumon, D. 1999. Comparative evolution of Jupiter and Saturn. Submitted to *Planet. Space Sci.*

Kippenhahn, R., Weigert, A. 1991. *Stellar Structure and Evolution*, Springer-Verlag, Berlin.

Klepeis, J.E., Schafer, K.J., Barbee, T.W., III, Ross, M. 1991. Hydrogen-helium mixtures at megabar pressures: Implications for Jupiter and Saturn. *Science* **254**, 986–989.

Landau, L., Lifchitz, E. 1984. *Physique statistique* (French translation), Editions Mir, Moscow.

Lécluse, C., Robert, F., Gautier, D., Guiraud, M. 1996. Deuterium enrichment in giant planets. *Plan. Space Sci.* **44**, 1579–1592.

Lindal, G.F., Wood, G.E., Levy, G.S., Anderson, J.D., Sweetnam, D.N., Hotz, H.B., Buckles, B.J., Holmes, D.P., Doms, P.E., Eshleman, V.R., Tyler, G.L., Croft, T.A. 1981. The atmosphere of Jupiter: An analysis of the Voyager radio occultation measurements. *J. Geophys. Res.* **86**, 8721–8727.

Lindal, G.F., Sweetnam, D.N., Eshleman, V.R. 1985. The atmosphere of Saturn: an analysis of the Voyager radio occultation measurements with Voyager 2. *J. Geophys. Res.* **92**, 14987–15001.

Lindal, G.F. 1992. The atmosphere of Neptune: An analysis of radio-occultations data acquired with Voyager 2. *Astron. Journal* **103**, 967–982.

Lissauer, J.J. 1993. Planet formation. *Annu. Rev. Astron. Astrophys.* **31**, 129–174.

Mahaffy, P.R, Donahue, T.M., Atreya, S.K., Owen, T.C., Niemann, H.B. 1998. Galileo probe measurements of D/H and ^{3}He/^{4}He in Jupiter's atmosphere. *Space Sci. Rev.* **84**, 251–263.

Marcy, G.W., Butler, R.P. 1998. Detection of extrasolar giant planets. *Ann. Rev. Astron. Astrophys.* **36**, 57–98.

Marley, M.S., Saumon, D., Guillot, T., Freedman, R.S., Hubbard, W.B., Burrows, A. & Lunine, J.I. 1996. On the nature of the brown dwarf Gliese 229 B. *Science* **272**, 1919–1921.

Mayor, M., Queloz, D. 1996. A Jupiter-mass companion to a solar-type star. *Nature* **378**, 355–359.

Nellis, W.J., Louis, A.A., Ashcroft, N.W. 1998. Metallization of fluid hydrogen. *Phil. Trans. R. Soc. Lond. A* **356**, 119-138.

Nellis, W.J., Weir, S.T., Mitchell, A.C. 1999. Minimum metallic conductivity of fluid hydrogen at 140 GPa (1.4 Mbar). *Phys. Rev. B* **59**, 3434–3449.

Niemann, H.B., Atreya, S.K., Carignan, G.R., Donahue, T.M., Haberman, J.A., Harpold, D.N., Hartle, R.E., Hunten, D.M., Kaspzrak, W.T., Mahaffy, P.R., Owen, T.C., Way, S.H. 1998. The composition of the jovian atmosphere as determined by the Galileo probe mass spectrometer. *Journal Geophys. Res.* **103**, 22831–22846.

Pfaffenzeller, O., Hohl, D., Ballone, P. 1995. Miscibility of hydrogen and helium under astrophysical conditions, *Phys. Rev. Lett.* **74**, 2599–2602.

Pollack, J.B., Hubickyj, O., Bodenheimer, P., Lissauer, J.J., Podolak, M., Greenzweig, Y. 1996. *Icarus* **124**, 62–85.

Roos-Serote M., Drossart, P., Encrenaz, T., Lellouch, E., Carlson, R.W., Baines, K.H., Kamp, L., Mahlman, R., Orton, G.S., Calcutt, S., Irwin, P., Taylor, F., Weir, A. 1998. Analysis of Jupiter north equatorial belt hot spots in the 4-5 μm range from Galileo/near-infrared mapping spectrometer observations: Measurements of cloud opacity, water and ammonia. *Journal Geophys. Res.* **103**, 23023–23042.

Roulston, M.S., Stevenson, D.J. 1995. Prediction of neon depletion in Jupiter's atmosphere *EOS* **76**, 343 [abstract].

Salpeter, E.E. 1973. On convection and gravitational layering in Jupiter and in stars of low mass. *Astrophys. J. Lett.* **181**, L183–L186.

Saumon D., Chabrier, G., Van Horn, H.M. 1995. An equation of state for low-mass stars and giant planets. *Astrophys. J. Suppl. Ser.* **99**, 713–741.

Saumon, D., Chabrier, G., Wagner, D.J., Xie, X. 1999. Probing the inner secrets of brown dwarfs and giant planets. preprint.

Seiff, A., Kirk, D.B., Knight, T.C.D., Young, R.E., Mihalov, J.D., Young, L.A., Milos, F.S., Schubert, G., Blanchard, R.C, Atkinson, D. 1998. Thermal structure of Jupiter's atmosphere near the edge of a 5-μm hot spot in the north equatorial belt. *Journal Geophys. Res.* **103**, 22857–22890.

Showman, A.P., Ingersoll, A.P. 1998. Interpretation of Galileo probe data and implications for Jupiter's dry downdrafts. *Icarus* **132**, 205–220.

Stevenson, D.J. 1982. Interiors of the giant planets. *Annu. Rev. Earth Planet. Sci* **10**, 257–295.

Stevenson, D.J. 1985. Cosmochemistry and structure of the giant planets and their satellites. *Icarus* **62**, 4–15.

Stevenson, D.J., Salpeter, E.E. 1977. The phase diagram and transport properties for hydrogen-helium fluid planets. *Astrophys. J. Suppl.* **35**, 221–237.

Thompson, S.L. 1990. ANEOS–Analytic equations of state for shock physics codes. Sandia Natl. Lab. Doc. SAND89-2951.

Weir, S.T., Mitchell, A.C., Nellis, W.J. 1996. Metallization of fluid molecular-hydrogen at 140 GPA (1.4 Mbar). *Phys. Rev. Lett.* **76**, 1860-1863.

von Zahn, U., Hunten, D.M., Lehmacher, G. 1998. Helium in Jupiter's atmosphere: results from the Galileo probe helium interferometer experiment. *J. Geophys. Res.* **103**, 22815–22830.

Zhang, K., Schubert, G. 1996. Penetrative convection and zonal flow on Jupiter. *Science* **273**, 941–943.

Zharkov V.N., Trubitsyn V.P. 1974. Determination of the equation of state of the molecular envelopes of Jupiter and Saturn from their gravitational moments. *Icarus* **21**, 152–156.

Zharkov V.N., Trubitsyn V.P. 1978. *Physics of planetary interiors*, W.B. Hubbard ed., Pachart Press, Tucson.

Zharkov, V.N., Gudkova, T.V. 1992. Modern models of giant planets. In *High Pressure Research: Application to Earth and Planetary Sciences* (Y. Syono and M.H. Manghgnani, Eds.), pp. 393–401.

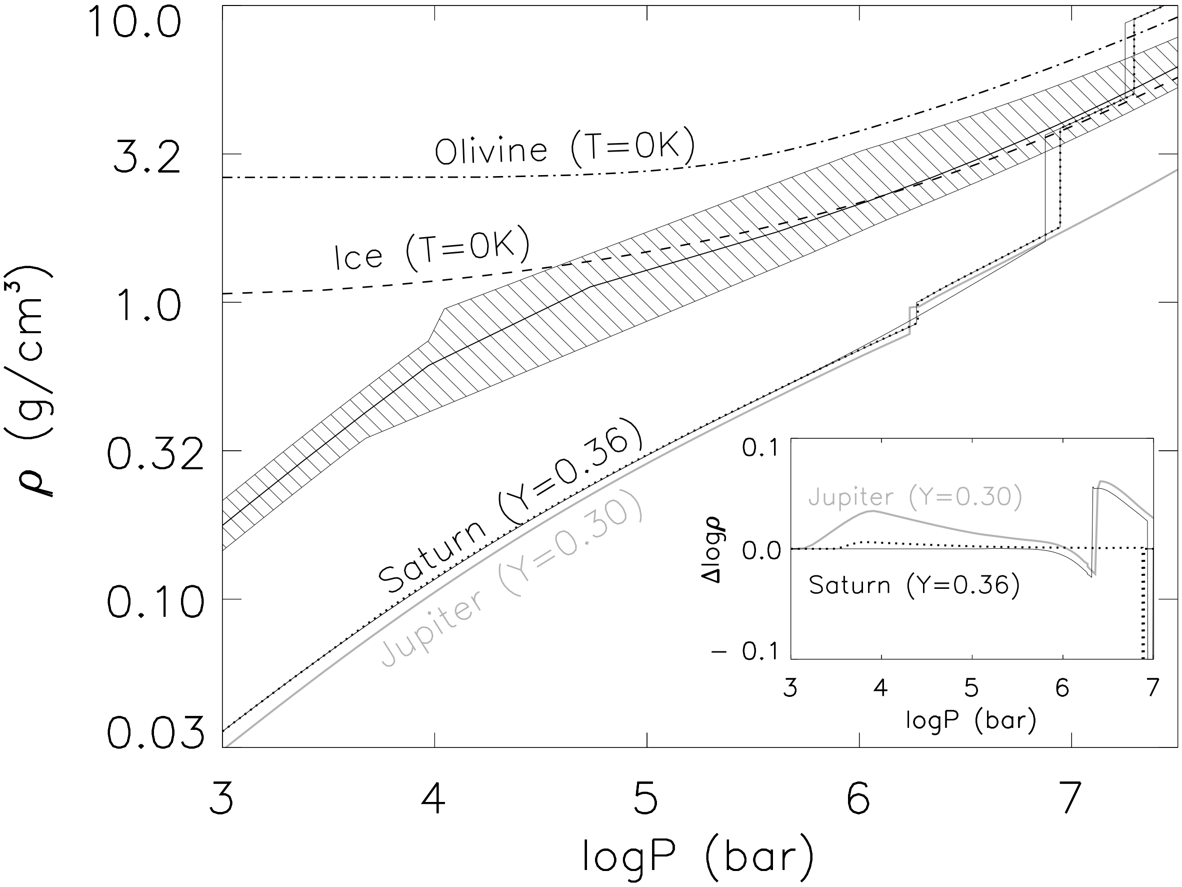

Figure 1: Density profiles in models of Jupiter (gray line) and Saturn (continuous lines: adiabatic i-EOS and PPT-EOS models; dashed: non-adiabatic i-EOS model). Upper curves (dashed and dot-dashed) are $T = 0$ K density profiles for water ice and olivine (from Thompson 1990). The dashed region represents the assumed uncertainty on the EOS for heavy elements ($\rho_Z(P,T)$). Within this region, the continuous line corresponds to our "preferred" profile for ρ_Z. *Inset*: Differences of the decimal logarithm of the Saturn density profiles with the same profile using the *i*-EOS and an adiabatic structure (plain and dotted lines). The gray line corresponds to the same difference but for a PPT-EOS non-adiabatic Jupiter model. (Adapted from Guillot et al. 1997).

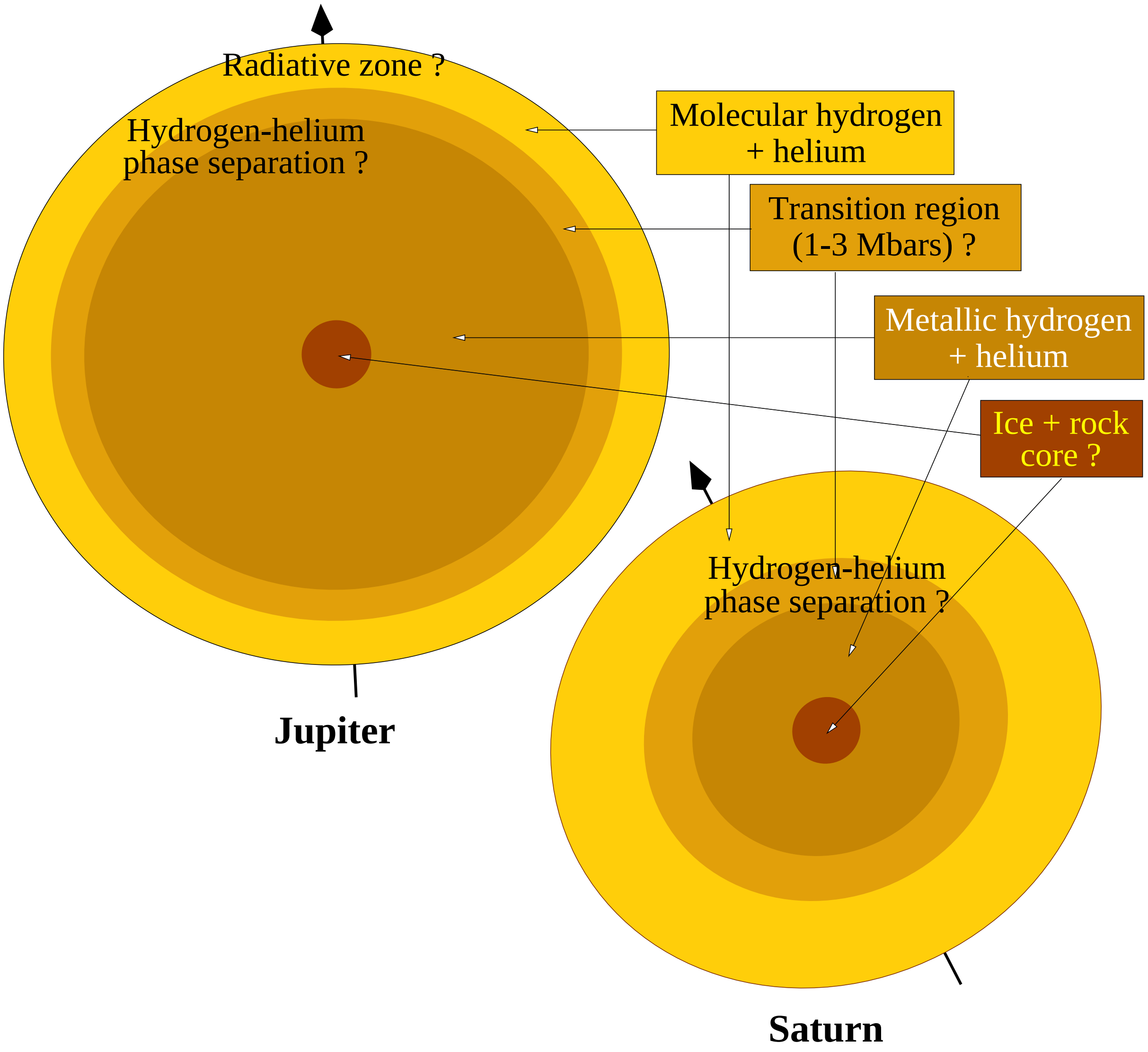

Figure 2: Conventional view of the interiors of Jupiter and Saturn, with a three-layer structure including the ice/rock core, the molecular and metallic regions. A transition region, assumed to lie between 1 and 3 Mbar, is represented, but experiments and theory are still unclear as to whether the separation between the molecular and metallic regions is sharp or not. The planets are shown to scale, with their observed oblateness and obliquity.

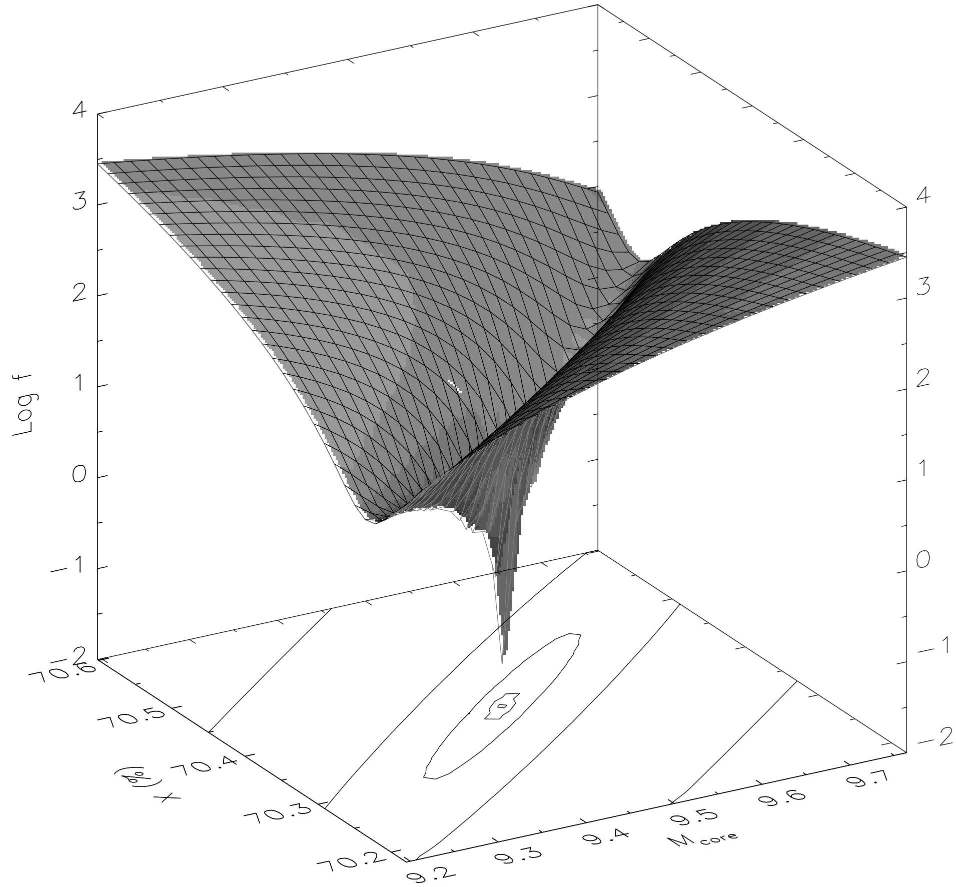

Figure 3: Optimization of a model of Jupiter. The surface represents the decimal logarithm of the minimization function χ^2 (see Eq. 9), as a function of the core mass $M_{\rm core}$ and the hydrogen mass mixing ratio $X = 1 - Y_Z$ in the molecular and metallic regions ($\Delta Y_Z = 0$). Each point of the χ^2 surface represents a converged interior model.

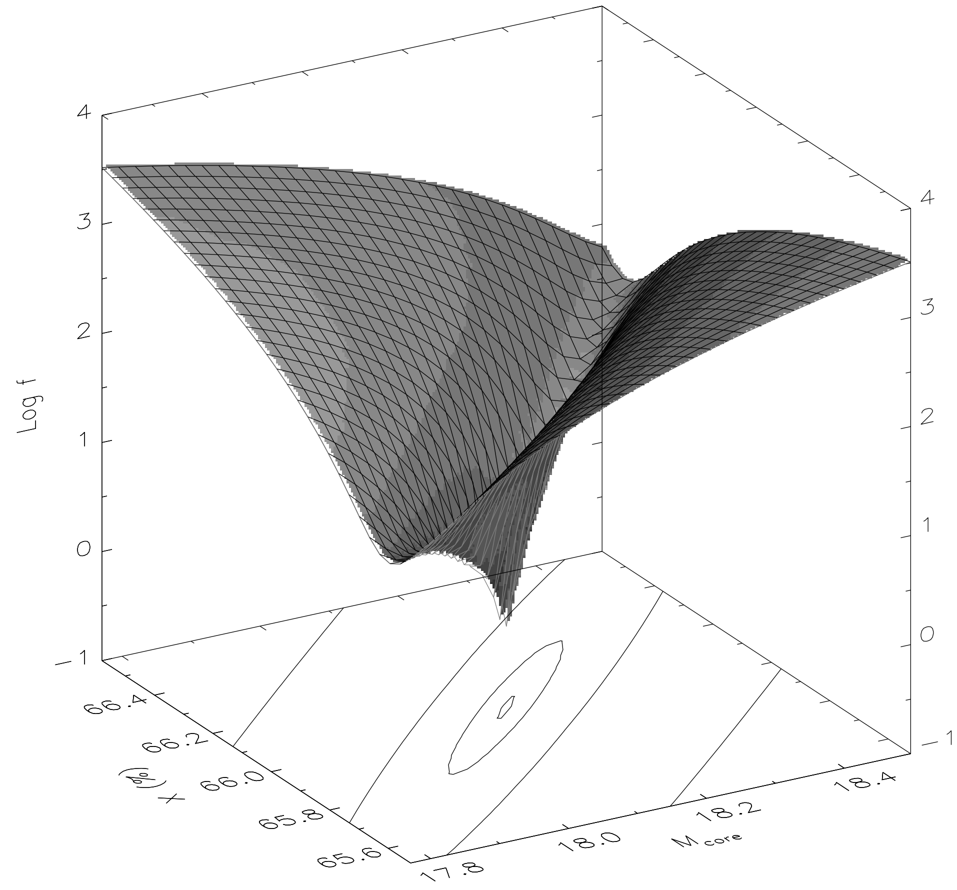

Figure 4: Same as Fig. 3 for a model of Saturn. Note that because one parameter is fixed ($\Delta Y_Z = 0$), the minimum found for $\chi^2(M_{\rm core}, Y_Z^{\rm mol})$ is still, in this case, 2.2σ away from the measured J_4.

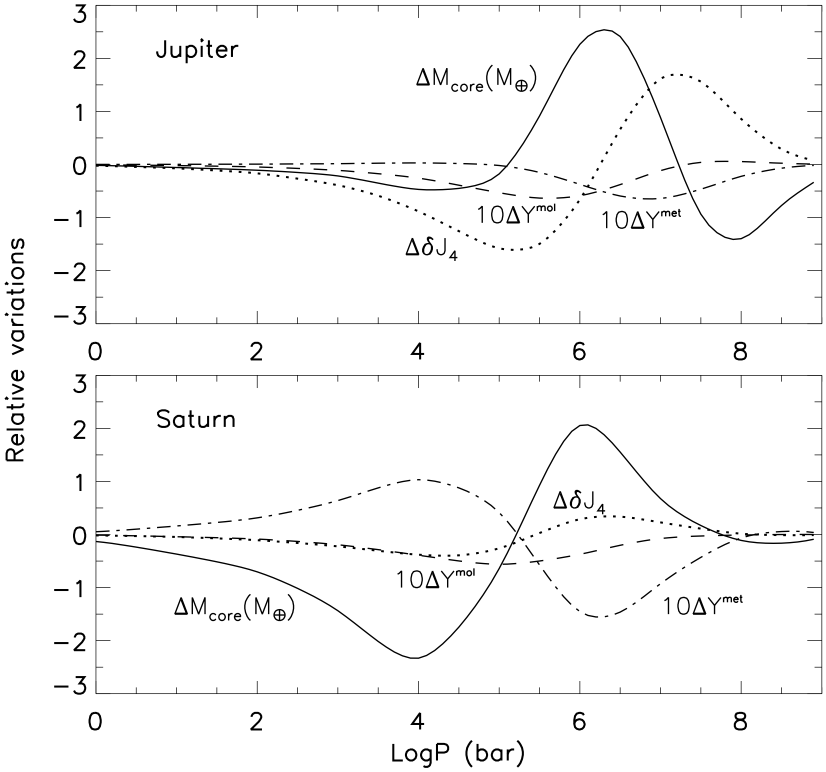

Figure 5: Variations of $\delta J_4 = [J_4 - J_4(\text{observed})]/\sigma_{J_4}$, $M_{\rm core}$ (in Earth masses), $Y_Z^{\rm mol}$ and $Y_Z^{\rm met}$ when the density at a given pressure P_0 (in abscissa) is increased by 5%. The increase is chosen to be a Gaussian in $\log(P/P_0)$ with a one-decade half-width. The variations of $Y_Z^{\rm mol}$ and $Y_Z^{\rm met}$ have been exaggerated by a factor 10.

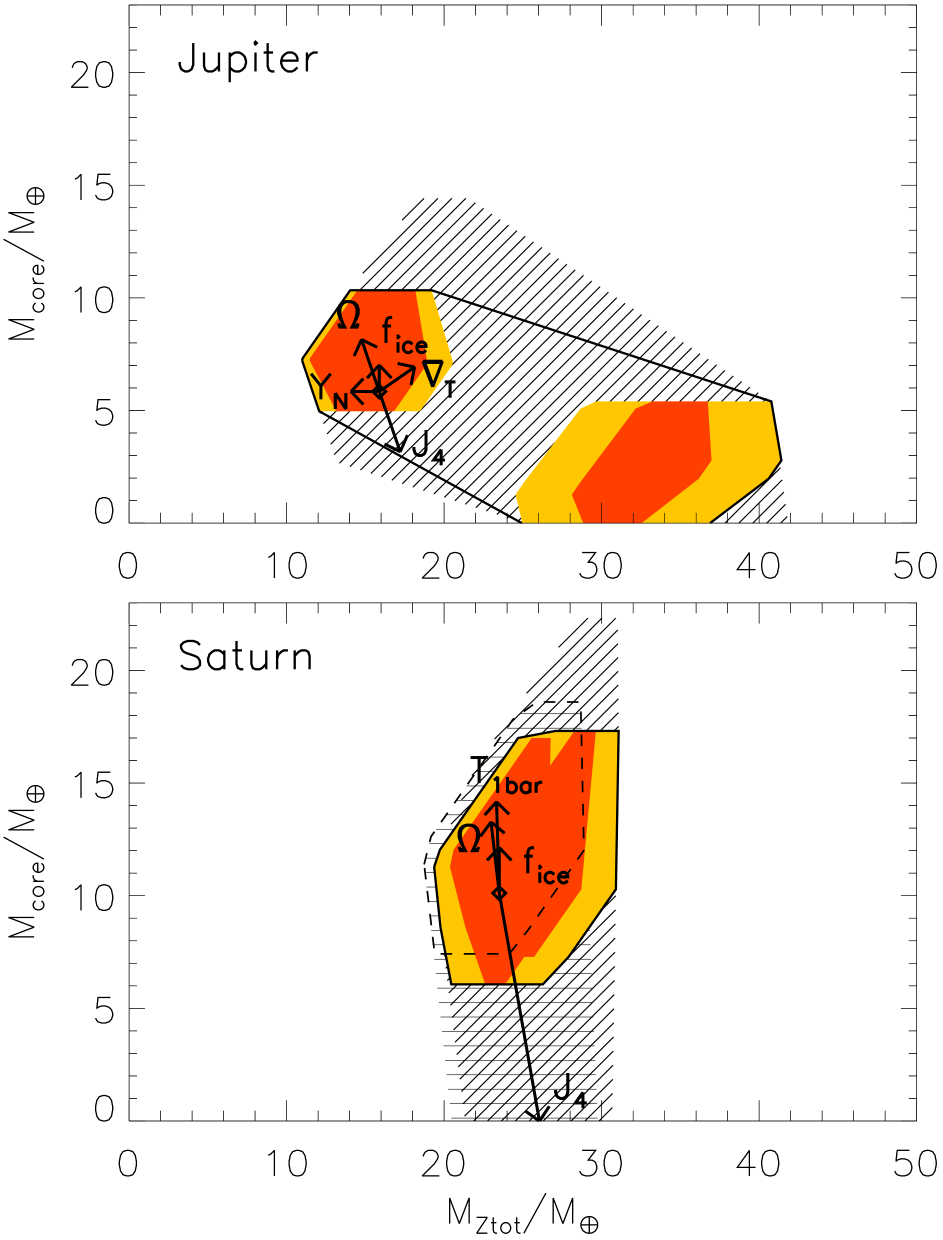

Figure 6: Constraints on Jupiter's (upper panel) and Saturn's (lower panel) core masses ($M_{\rm core}$) and total masses of heavy elements ($M_{Z{\rm tot}}$), expressed in Earth masses ($M_\oplus$). The dashed regions correspond to the constraints obtained from static models only. The shaded regions are those which also satisfy the condition that the model ages should be close to the age of the Solar System (see text). Within those, darker regions corresponds to calculations that ignore uncertainties on the equation of state of heavy elements. Models calculated with the PPT-EOS are to the left, models using the *i*-EOS to the right. The region surrounded by the thick line corresponds to the most plausible ($M_{\rm core}$, $M_{Z{\rm tot}}$) region given all possible constraints and uncertainties. In the case of Saturn, the horizontally-dashed region and the region surrounded by dashed lines correspond to constraints using the Voyager helium mixing ratios $Y = 0.06 \pm 0.05$, whereas other models assume $Y = 0.16 \pm 0.05$. Arrows indicate the direction and magnitude of the assumed uncertainties, if J_4 or $Y_{\rm proto}$ are increased by 1σ, rotation is assumed to be solid ("Ω"), the core is assumed to be composed of ices only ("$f_{\rm ice}$"), if Jupiter's interior becomes fully adiabatic ("∇_T"), and if Saturn's surface temperature is increased from 135 to 145 K ("$T_{\rm 1bar}$").

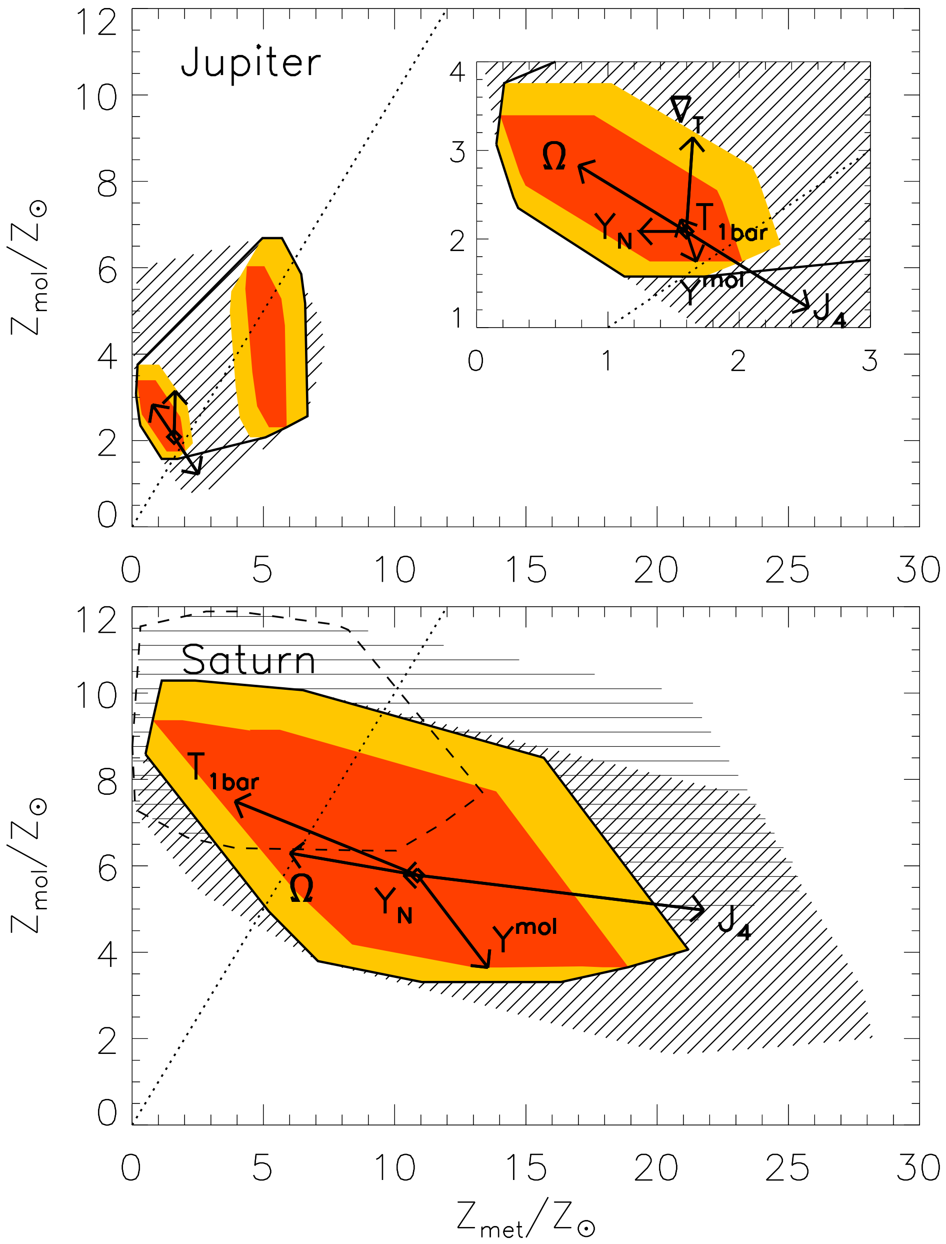

Figure 7: Same as Fig. 6 but for constraints on the mass fractions of heavy elements in the molecular envelope ($Z_{\rm mol}$), and in the metallic envelope ($Z_{\rm met}$). The $Z_{\rm mol} = Z_{\rm met}$ relations are shown by diagonal dotted lines. Additional arrows not included in Fig. 6 show the changes due to a 1-σ increase in the surface helium mass mixing ratio ("$Y^{\rm mol}$"), and in the case of Jupiter, of an increase in surface temperature from 165 to 170K ("$T_{\rm 1bar}$"). The mixing ratios are in solar units ($Z_\odot = 0.0192$; see Anders & Grevesse 1989). *Inset*: closeup view of the solutions and assumed uncertainties for Jupiter models calculated with the PPT-EOS.

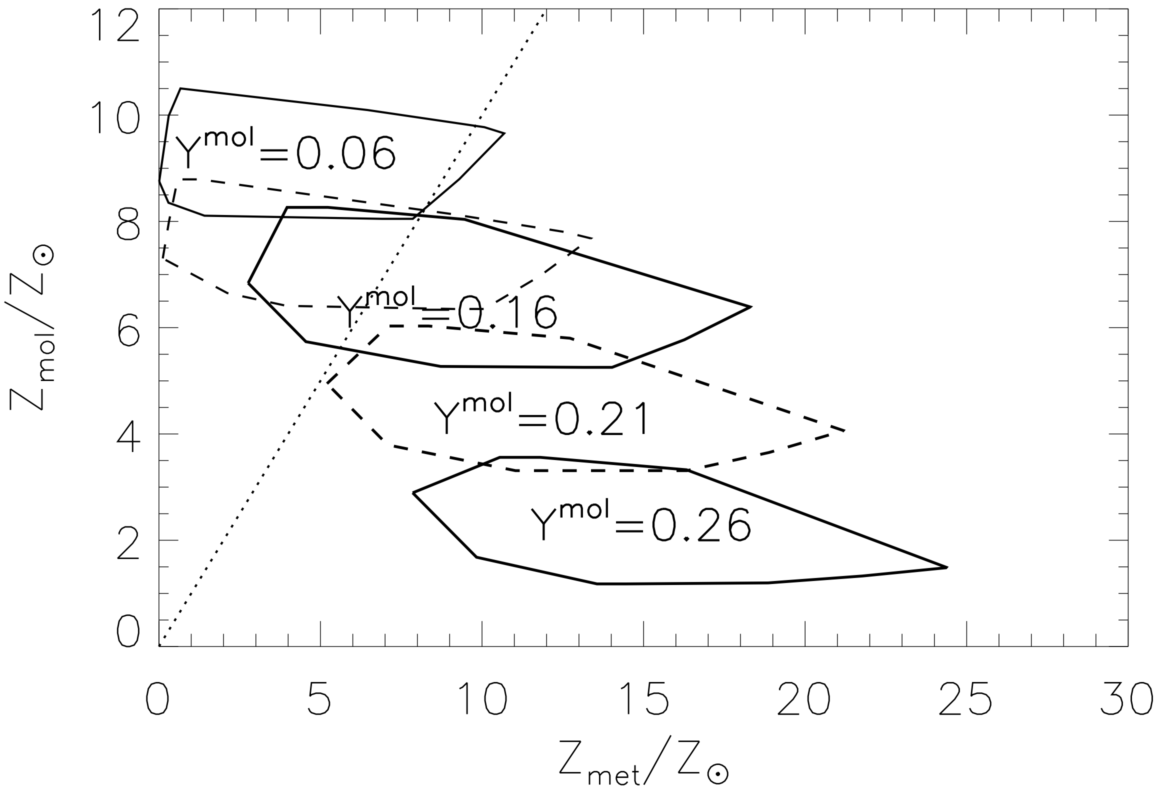

Figure 8: Same as Fig. 7 but for Saturn only. The ensemble of solutions shown represent models matching gravitational *and* age constraints for given surface helium mass mixing ratios, from $Y^{\rm mol} = 0.06$ to 0.26, as indicated (except for $Y^{\rm mol} = 0.11$, between $Y^{\rm mol} = 0.06$ and 0.16). Observations of the abundances of chemical species in Saturn's atmosphere tend to favor higher values of $Y^{\rm mol}$ than indicated by Voyager ($Y = 0.06 \pm 0.05$).

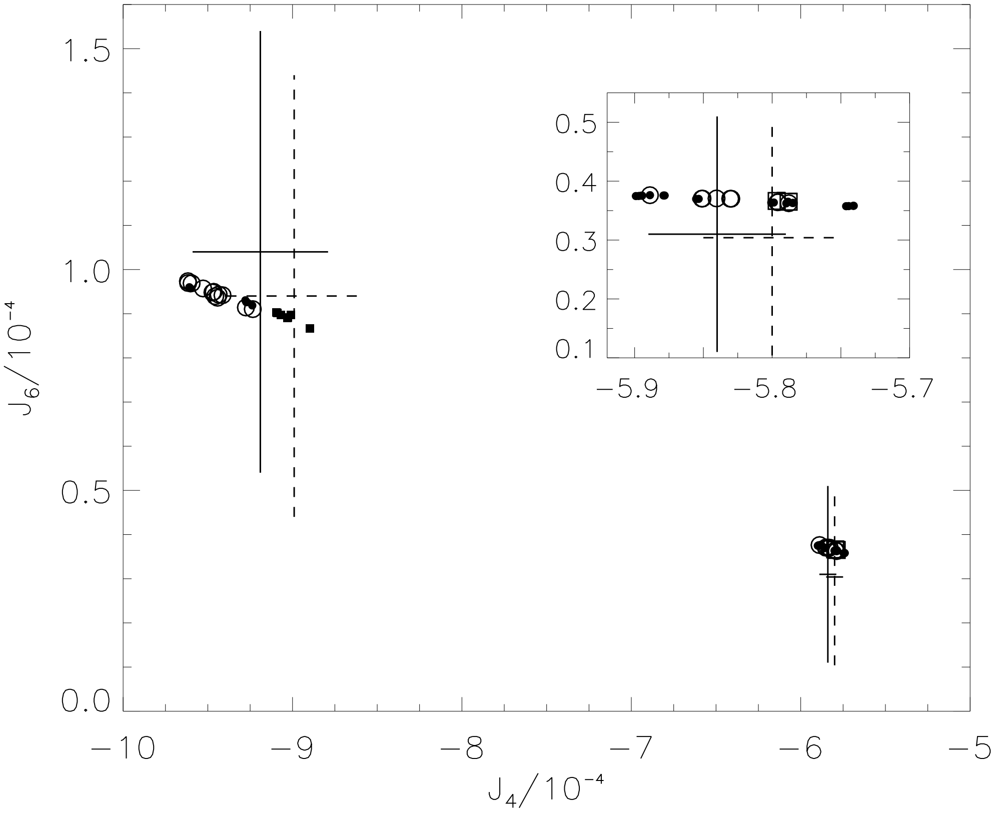

Figure 9: Gravitational moments J_4 and J_6 of the optimized models of Jupiter (right) and Saturn (left). Large open symbols represent models that satisfy all constraints. Small filled symbols represent models that match the observed gravitational field but do not predict ages in agreement with that of the Solar System. Squares are models with *no* core, all other models being represented by circles. The plain crosses are the observational constraints on (J_4, J_6). The dashed crosses show the constraints derived when differential rotation is assumed to reach the deep interior. Inset is an enlargement of the solutions obtained for Jupiter.

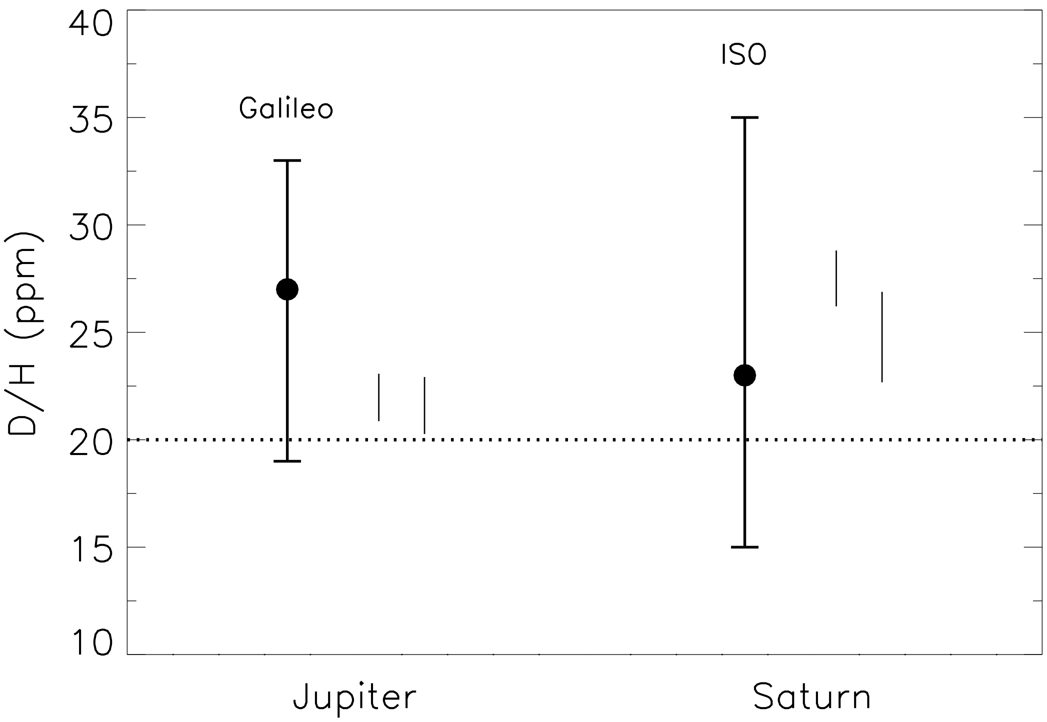

Figure 10: Observational and theoretical isotopic D/H ratio in Jupiter and Saturn, in parts per million (ppm). The measurements from Galileo in Jupiter and ISO in Saturn are shown with their error bars. Theoretical estimates (thin lines) are calculated assuming that ice carriers had a D/H similar to that observed in comets (300 ppm). The lines that are to the left assume that the central core exchanged its deuterium with the envelope, the lines to the right (which predict slightly smaller D/H values) assume that such exchange didn't take place because of convection inhibition at the core/envelope boundary. The assumed protosolar D/H ratio used for the calculation (20 ppm) is shown as a dotted line. The additional uncertainty on the protosolar value was not taken into account. Its value is inferred from the ^{3}He/^{4}He ratio in the solar wind, and amounts to 21 ± 5 ppm (Geiss & Gloecker, 1998). Deuterium enrichment on Jupiter and Saturn is hence not detectable yet.